ANNUAL REVIEWS

Annual Review of Pathology: Mechanisms of Disease

Comparative Pathogenesis of Severe Acute Respiratory Syndrome Coronaviruses

Jingshu Zhang,* Melanie Rissmann,* Thijs Kuiken, and Bart L. Haagmans

Viroscience Department, Erasmus Medical Center, Rotterdam, The Netherlands; email: b.haagmans@erasmusmc.nl

Annu. Rev. Pathol. Mech. Dis. 2024. 19:423–51

First published as a Review in Advance on October 13, 2023

The *Annual Review of Pathology: Mechanisms of Disease* is online at pathol.annualreviews.org

https://doi.org/10.1146/annurev-pathol-052620-121224

*These authors contributed equally to this article

Keywords

SARS-CoV, SARS-CoV-2, COVID-19, pathogenesis, viral transmission

Abstract

Over the last two decades the world has witnessed the global spread of two genetically related highly pathogenic coronaviruses, severe acute respiratory syndrome coronavirus (SARS-CoV) and SARS-CoV-2. However, the impact of these outbreaks differed significantly with respect to the hospitalizations and fatalities seen worldwide. While many studies have been performed recently on SARS-CoV-2, a comparative pathogenesis analysis with SARS-CoV may further provide critical insights into the mechanisms of disease that drive coronavirus-induced respiratory disease. In this review, we comprehensively describe clinical and experimental observations related to transmission and pathogenesis of SARS-CoV-2 in comparison with SARS-CoV, focusing on human, animal, and in vitro studies. By deciphering the similarities and disparities of SARS-CoV and SARS-CoV-2, in terms of transmission and pathogenesis mechanisms, we offer insights into the divergent characteristics of these two viruses. This information may also be relevant to assessing potential novel introductions of genetically related highly pathogenic coronaviruses.

1. INTRODUCTION

Coronaviruses are common pathogens of animals and humans. In the past two decades two zoonotic coronaviruses, both belonging to the genus *Sarbecovirus*, emerged and caused significant mortality in humans. Severe acute respiratory syndrome coronavirus (SARS-CoV) originated in Guangdong, China, in 2002 and caused an outbreak with 8,096 confirmed cases and 774 deaths in 29 countries (1). Although bats are considered the natural reservoir for SARS-CoV-like viruses, civets and raccoon dogs are the incidental intermediate hosts (2, 3). This devastating outbreak thus drew attention to the potential cross-species transmission of coronaviruses and raised concerns about the reemergence of related SARS-CoVs and other coronaviruses (4). In late 2019, a novel human coronavirus was detected in Wuhan, China, in a cluster of patients with pneumonia (5). The emergence of this virus, named SARS-CoV-2 (6), eventually resulted in the coronavirus 2019 disease (COVID-19) pandemic. Current scientific evidence supports the hypothesis that, similar to SARS-CoV, SARS-CoV-2 also has a zoonotic origin (7–9), affirming the previous concerns about the potential emergence of new coronaviruses and spillover into the human population (4). However, unlike the SARS-CoV outbreak, which was quickly contained through public health measures, SARS-CoV-2 led to a pandemic of unprecedented scale, causing more than 769 million confirmed infections and more than 6.9 million confirmed deaths worldwide (status as of 9 August 2023). The precise cause behind the vastly distinct outbreak outcomes of SARS-CoV and SARS-CoV-2 is not well understood. These two viruses share 79% genomic similarity, both use angiotensin-converting enzyme 2 (ACE2) as the cellular receptor (10–15), and both replicate in the lower respiratory tract, with the capability to cause a potentially fatal acute respiratory distress syndrome (ARDS) (16, 17). However, the fatality rate of SARS-CoV was notably higher (~10%) (1) compared with SARS-CoV-2 during the initial phase of the outbreak (less than 1%) (18) (**Table 1**). In addition, variations in infection kinetics and viral shedding were observed for these two viruses. Unlike those infected with SARS-CoV, individuals infected with SARS-CoV-2 could transmit the virus even before symptom onset, allowing for asymptomatic transmission (19). Given the fact that the emergence of novel coronaviruses in humans is quite likely, a further understanding of the characteristics and determinants of pathogenicity of SARS-CoVs is crucial for future pandemic preparedness. To address this, we provide a comprehensive review on the comparative pathogenesis of SARS-CoV-2 and SARS-CoV, with a particular focus on the infection of the respiratory tract in immunologically naive hosts. By summarizing the key features of pathology in humans and animals, as well as mechanisms of pathogenesis, we explore what makes SARS-CoV-2 a unique pandemic causative agent.

2. PATHOLOGICAL OBSERVATIONS

2.1. Pathological Changes in the Human Respiratory Tract

The main pathological changes seen in humans infected with SARS-CoVs are observed in the respiratory tract. Both SARS-CoV and SARS-CoV-2 infections can cause ARDS, as postmortem examinations of lung tissues from fatal human cases revealed significant pathological characteristics related to this condition (16, 17) (**Table 1**).

In SARS-CoV patients, the lungs were heavy and edematous and showed consolidation. In some cases, there was diffuse consolidation and mucopurulent material in the tracheobronchial tree (20, 21). The main lesion in SARS-CoV postmortem lungs was diffuse alveolar damage (DAD), characterized by flooding of alveolar lumina with edema fluid, epithelial denudation of alveolar walls, and formation of hyaline membranes along alveolar walls. Many alveoli collapsed, and those remaining were filled with fluid and desquamated alveolar and bronchiolar epithelial cells. Both hypertrophy and hyperplasia of alveolar type II pneumocytes (AT2 cells) were

Table 1 General characteristics of SARS-CoV and SARS-CoV-2

		SARS-CoV	SARS-CoV-2
Outbreak scale			
Case numbers		8,096 confirmed cases; 774 deaths (1)	769 million confirmed cases; more than 6.9 million confirmed deaths
Fatality rate		~10% (1)	Less than 1% (18)
Key clinical/pathological observations in human respiratory tract			
Viral shedding		5–15 days after symptoms onset (42)	0–12 days after symptoms onset (44)
Severe complications		ARDS, hypercytokinemia (16)	ARDS, hypercytokinemia (17)
Pathological observations		DAD, hypertrophy and hyperplasia of AT2 cells, squamous metaplasia, infiltration of immune cells, pulmonary fibrin thrombi (20, 21)	DAD, hyperplasia of AT2 cells, squamous metaplasia, infiltration of immune cells, pulmonary microthrombus (22)
Key clinical/pathological observations in animal respiratory tracts			
Hamster	Viral shedding	2–14 dpi (24)	2–14 dpi (27)
	Clinical/pathological observations	No obvious clinical signs; pulmonary consolidation; mononuclear infiltrates in nose and bronchioles; alveolar immune cell infiltration; viral titers higher in lungs than in nose (24–26)	Body weight loss and lethargy; pulmonary consolidation, edema and necrosis, submucosal immune cell infiltration; viral titers higher in nose than in lungs (29–31)
NHPs	Viral shedding	5–11 dpi (34)	2–8 dpi (37)
	Clinical/pathological observations	Lethargy and fever (highly variable); pulmonary consolidation; DAD with edema, necrosis, hyaline membranes, syncytia, and AT2 cell hyperplasia (25, 26, 35)	No or mild symptoms (highly variable, age dependent); pulmonary consolidation; multifocal interstitial pneumonia with edema, necrosis, hemorrhage, syncytia, and AT2 cell hyperplasia (29–31)
Ferret	Viral shedding	2–14 dpi (38)	2–14 dpi (29)
	Clinical/pathological observations	Lethargy and fever; partially lethal; mild alveolar necrosis, edema, and lymphocytic infiltration; lymphohistiocytic bronchopneumonia; viral replication in trachea and lungs (25, 26, 35)	No or mild symptoms; eosinophilic rhinitis; pulmonary perivasculitis and vasculitis; eosinophilic alveolar inflammation; viral replication only in nasal turbinates (29)
Molecular characteristics			
Cellular receptor		ACE2 (102)	ACE2 (103)
Cellular protease(s)		TMPRSS2 (11)	TMPRSS2, furin (10)

Abbreviations: ACE2, angiotensin-converting enzyme 2; ARDS, acute respiratory distress syndrome; AT2, alveolar type II pneumocyte; DAD, diffuse alveolar damage; dpi, days post-infection; NHP, non-human primate; SARS-CoV, severe acute respiratory syndrome coronavirus; TMPRSS2, transmembrane serine protease 2.

observed. Hypertrophic AT2 cells exhibited cytomegaly (unusually large in size), enlarged nuclei with prominent nucleoli, and granular cytoplasm. Alveolar macrophages (CD68-positive) showed mild to moderate increase, with some demonstrating hemophagocytosis. Multinucleated giant cells (syncytia), derived from macrophages (CD68-positive) or epithelium (AE1/3-positive), were present in some cases. Additional observations in these lung tissues included fibrin thrombi in pulmonary blood vessels, intimal swelling of pulmonary blood vessels, small vessel vasculitis, and a paucity of lymphocytic or other inflammatory cell infiltration (20, 21).

In fatal COVID-19 cases, the lungs were heavy, edematous, and displayed variable pleural fluid volume. Central pulmonary emboli, intraparenchymal hemorrhage, and pulmonary consolidation were also observed (22). DAD was often observed in COVID-19 lungs as well, ranging from acute to organizing stages, characterized by the presence of intra-alveolar fibrin, hyaline membranes,

or loosely organizing connective tissue in alveolar septa. Similar to fatal SARS-CoV infection, large syncytia were present in lumen of alveoli and airways in these COVID-19 lungs. However, these syncytia were confirmed to be of epithelial (TTF-1-positive) rather than macrophage (CD68-positive) origin on the basis of immunohistochemistry (IHC). Most cases had variable degrees of chronic interstitial inflammation, including perivascular lymphocytic infiltrates, as well as variable neutrophilic infiltrates. Microscopic hemorrhage with DAD was noted in some cases. There was mild tracheitis, characterized by edema and small lymphocytic aggregates in the tracheal submucosa (22). Areas of pulmonary necrosis, microthrombi, pulmonary megakaryocytes, and endotheliitis were also observed (23).

2.2. Pathological Changes in Animal Respiratory Tracts

To study SARS-CoV pathogenesis in a more controlled setting, several animal models have been developed. The emergence of the SARS-CoV epidemic has driven significant research efforts in the past decades to identify suitable animal models, a need that has become even more pressing during the SARS-CoV-2 pandemic. An ideal animal model is permissive for viral infection and mirrors clinical manifestation, immunological responses, and pathological changes of human patients.

2.2.1. Hamsters. Syrian golden hamsters are nowadays the most suitable small animal model for infections with SARS-CoV and SARS-CoV-2. Neither genetic adaptations of the animal nor adaptations of the viruses are needed, and animals are characterized by their high permissiveness for viral infection (**Figure 1**) (**Table 1**).

Hamsters infected with SARS-CoV did not exhibit obvious clinical disease, although mortality was reported in one study with 3 out of 20 hamsters that died after infection with SARS-CoV (strain Frankfurt-1). SARS-CoV replicated extensively in nasal turbinates and lungs, peaking at 2–3 days post-infection (dpi), and was cleared from lungs by 7 dpi and from nasal turbinates by 14 dpi. Viral titers in nasal turbinates were 10- to 100-fold lower compared with lungs. At postmortem examination, consolidated areas of up to 40% were found in the lungs, along with swelling of epithelial cells, ulceration, and cellular debris accumulation. Tracheitis with loss of cilia and bronchiolitis were also detected. Additionally, mononuclear cell infiltrates were found in submucosa of nasal epithelium and bronchioles. In the lower respiratory tract, pulmonary consolidation and inflammatory infiltrates in the alveolar septa were found. SARS-CoV viral antigens were detected in respiratory epithelium and endothelial cells of the nasal turbinates, submucosal glands, tracheal epithelium, and, to a lesser extent, pneumocytes and pulmonary endothelial cells (24–26).

SARS-CoV-2-infected hamsters commonly experienced body weight loss of up to 20%, marking acute viral replication and pulmonary changes. Additionally, lethargy, ruffled fur, hunched posture, and respiratory distress were observed to variable extent. Radiological findings typically included ground-glass opacities, dilated airways, and pulmonary consolidation. Proinflammatory cytokines, such as interferon-gamma (IFNγ), interleukin-6 (IL6), IL10, and tumor necrosis factor-alpha (TNFα), were commonly induced. Unlike in humans, there was no upregulation of transforming growth factor-beta (TGFβ), a key factor for pulmonary fibrosis, in hamsters up to 14 dpi. Viral replication in the respiratory tract peaked 2–3 dpi and was usually cleared by 14 dpi. Infectious virus level was 1–2 logs higher in nasal turbinates than in the lungs, peaking between 2–4 dpi (27). Pathological findings in SARS-CoV-2-infected hamsters indicated pulmonary consolidation, edema, and various respiratory tract abnormalities such as epithelial necrosis, inflammation, blood vessel congestion, submucosal infiltration of immune cells, and accumulation of cellular debris. An upregulation of lung injury markers was found in SARS-CoV-2-infected

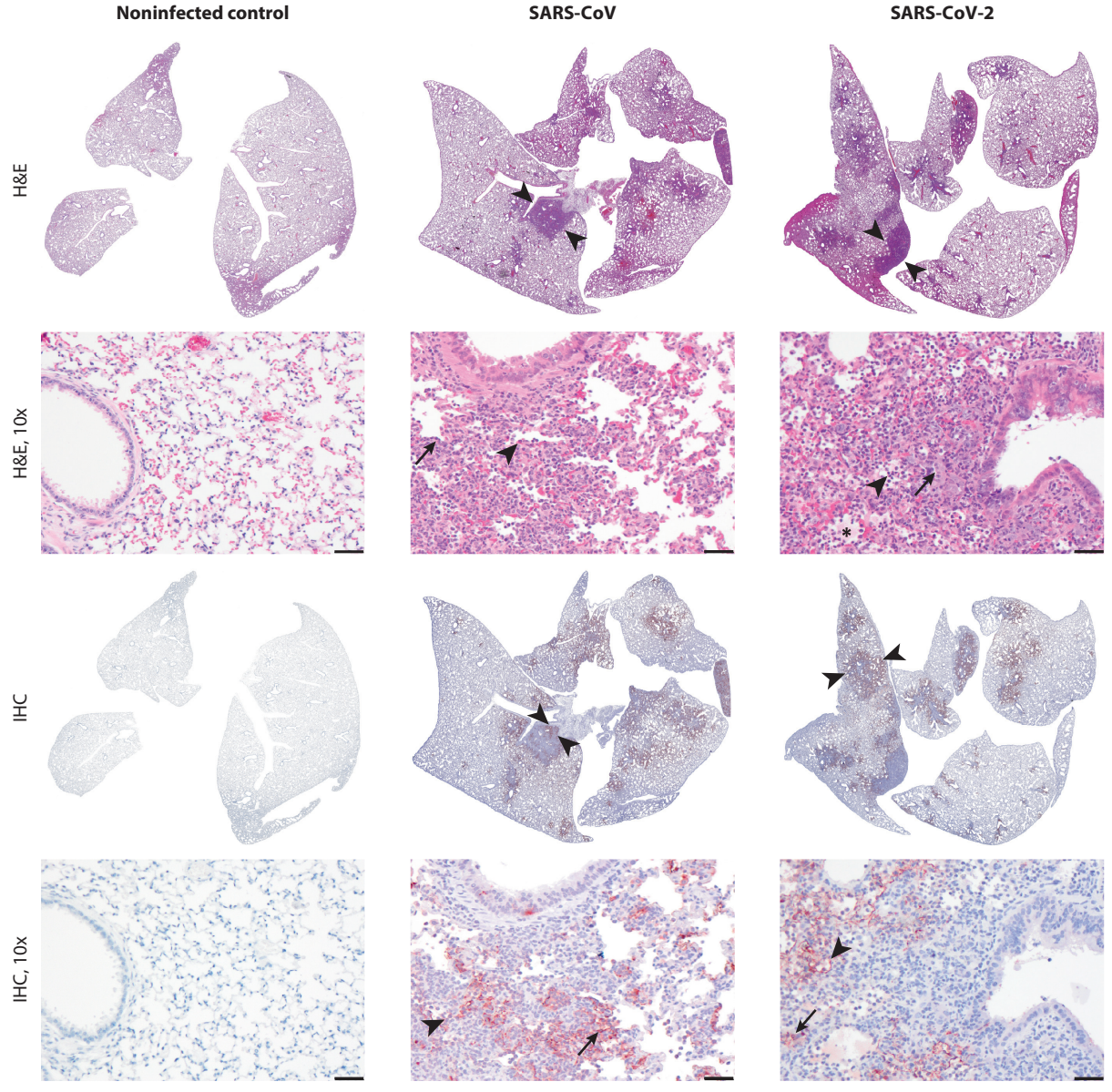

Figure 1

Pathological findings in lungs of Syrian golden hamsters infected with SARS-CoV or SARS-CoV-2. The figure shows histopathological changes and viral antigen expression in the lungs of noninfected Syrian golden hamsters and hamsters that were inoculated with SARS-CoV (strain HKU39849) or SARS-CoV-2 (strain Germany/BavPat1/2020) at a titer of 10^6 $TCID_{50}$/animal and were euthanized at 4 dpi. Viral nucleocapsid protein was stained with IHC. (*First row*) Compared with noninfected controls, the lungs of SARS-CoV- and SARS-CoV-2-inoculated hamsters have multiple foci of inflammation (between *arrowheads*) in the lungs, which consist of (*second row*) flooding of the alveolar lumina with edema fluid (*asterisk*), influx of neutrophils (*arrowheads*), and hyperplasia of alveolar type II pneumocytes (*arrows*). (*Third row*) The foci of inflammation are colocalized with viral nucleocapsid protein expression (between *arrowheads*), visible as brown staining. (*Fourth row*) Cells expressing viral nucleocapsid protein are both alveolar type I pneumocytes (*arrowheads*) and alveolar type II pneumocytes (*arrows*). Bars indicate 50 μm. Abbreviations: dpi, days post-infection; H&E, hematoxylin and eosin; IHC, immunohistochemistry; SARS-CoV, severe acute respiratory syndrome coronavirus; $TCID_{50}$, 50% tissue culture infectious dose. Tissues originated from M. Rissmann, E.J.B. Veldhuis Kroeze, P. van Run, A. Mykytyn, D. van Eck Schipper, et al., unpublished work.

hamsters, accompanied by AT2 cell hyperplasia, syncytia, and fibrin strands. Viral antigens were found in bronchiolar epithelial cells, AT1 and AT2 cells, and basal and sustentacular cells of the olfactory epithelium in the nasal turbinates (28). Single-cell RNA sequencing (scRNA-seq) of SARS-CoV-2-infected hamster lungs revealed that macrophages and neutrophils were the dominant infiltrating cell populations, with macrophages containing the most viral particles and being prime drivers of virus elimination. Vascular injury signs were commonly observed, but thrombi were absent in the lungs of infected hamsters (29–31). In addition to Syrian golden hamsters, the Roborovski dwarf hamster (*Phodopus roborovskii*), displaying severe clinical symptoms and acute DAD, provides an alternative model for studying SARS-CoV-2 (32).

Studies directly comparing the outcomes of SARS-CoV and SARS-CoV-2 infections in Syrian golden hamsters are lacking to date. While detailed data for SARS-CoV are currently limited, there is an indication of more pronounced viral replication in the nose of SARS-CoV-2-infected hamsters. However, no significant differences were observed in the comparative pathology of the lower respiratory tract (**Figure 1**) (**Table 1**).

2.2.2. Non-human primates. Non-human primates (NHPs) offer the great advantage of close resemblance to humans in terms of anatomy, physiology, and immunology. Several NHP species were recruited in studies with SARS-CoV and SARS-CoV-2, with rhesus macaques (*Macaca mulatta*), cynomolgus macaques (*Macaca fascicularis*), and African green monkeys (*Chlorocebus aethiops*) being the most commonly used.

Clinical manifestations in NHPs after infection with SARS-CoV varied extensively between different experiments and included lethargy, transient fever, diarrhea, and rare progression to ARDS. Radiological examinations revealed multifocal pneumonia peaking at 8–10 dpi (33). Viral replication in the lungs was observed between 4–7 dpi, followed by an early clearance phase starting at 4 dpi. Macroscopic lesions were characterized by a species-specific extent of multifocal pulmonary consolidation. Necrosis of bronchiolar epithelium and multifocal tracheitis and bronchitis with lesions in the submucosal glands were observed. Histopathological changes exhibited variability, encompassing a range of manifestations including DAD, diffuse mild interstitial edema, alveolar inflammation and necrosis, thickening of alveolar walls, hyaline membranes, syncytia, AT2 cell hyperplasia, and infiltration of lymphocytes and macrophages. These changes were observed between 5 and 60 dpi, with signs of active recovery in later stages of infection (34). Viral antigens were detected in AT1 and AT2 cells and alveolar macrophages, as well as bronchiolar, bronchial, and tracheal epithelial cells (25, 26, 35).

After infection with SARS-CoV-2, NHPs usually show no or mild symptoms with a high interindividual variation. Of those clinical signs, loss of appetite, weight loss, and lethargy were the most commonly observed. A progression to acute ARDS was barely observed in aged animals (36). Radiological findings were dominated by edema, consolidation, and ground-glass opacities, indicative of interstitial pneumonia. Hematological analyses revealed monocytosis, neutrophilia, and lymphopenia. Proinflammatory chemo- and cytokines were elevated in respiratory samples [e.g., IL6, IL10, IFNα, IFNγ, TNFα, and C-X-C motif chemokine ligand 10 (CXCL10)]. Viral replication was initiated in the upper respiratory tract, peaking at 1–3 dpi, and followed by progression to the lower respiratory tract up to 18 dpi. Typically, recovery was observed between 9–17 dpi. Macroscopic pulmonary changes in SARS-CoV-2-infected NHPs included foci of consolidation, hyperemia, and hemorrhage. Rhinitis, tracheitis, bronchitis, and bronchiolitis with infiltration of mononuclear cells, necrosis, and inflammation were detected in the respiratory tract. Histopathologic changes were characterized by a multifocal or diffuse interstitial pneumonia with cellular necrosis, alveolar septal thickening, edema, fibrin deposition, hemorrhage, and perivascular cuffing. Hyperplasia of AT2 cells and syncytia could be found regularly, whereas hyaline membranes

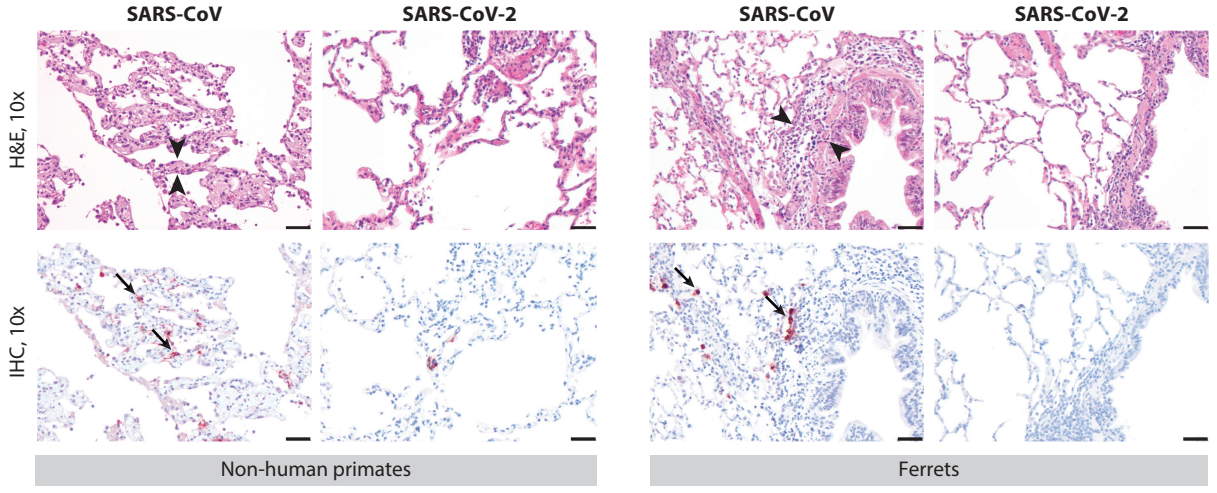

Figure 2

Comparison of pathological findings in lungs of non-human primates and ferrets infected with SARS-CoV or SARS-CoV-2. The figure shows histopathological changes and viral antigen expression in the lungs of cynomolgus macaques and ferrets that were inoculated with SARS-CoV (strain HKU39849) or SARS-CoV-2 (strain Germany/BavPat1/2020) with 10^6 $TCID_{50}$/animal (cynomolgus macaques) or 10^5 $TCID_{50}$/animal (ferrets) and were euthanized at 4 dpi. Viral nucleocapsid protein was stained with IHC. Thickening of alveolar walls (between *arrowheads*) and more pronounced viral antigen presence (*arrows*) can be observed in SARS-CoV-infected macaques. In comparison, alveolar wall thickening is less pronounced and only occasional viral antigens can be found in SARS-CoV-2-infected macaques. Peribronchiolar accumulation of neutrophils and lymphocytes (between *arrowheads*) and enhanced presence of viral antigens (*arrows*) are observed in SARS-CoV-infected ferrets. Neither viral antigens nor obvious lesions are observed in the lungs of SARS-CoV-2-infected ferrets. Bars indicate 50 μm. Abbreviations: dpi, days post-infection; H&E, hematoxylin and eosin; IHC, immunohistochemistry; SARS-CoV, severe acute respiratory syndrome coronavirus; $TCID_{50}$, 50% tissue culture infectious dose. Cynomolgus macaque tissues were retrieved from previous studies (37, 148). Ferret tissues originated from M. Rissmann, E.J.B. Veldhuis Kroeze, P. van Run, A. Mykytyn, D. van Eck Schipper, et al., unpublished work.

were rarely observed. Infiltrating cells were dominated by macrophages and neutrophils. Viral antigens can be found in AT1 and AT2 cells, upper respiratory and conducting airway epithelial cells, and alveolar macrophages. Endotheliitis, vasculitis, and pulmonary microthrombi were described occasionally (29–31).

No significant distinctions were reported in clinical manifestation, tissue and cell tropism, or histopathological changes between SARS-CoV- and SARS-CoV-2-infected NHPs, considering the high degree of interindividual variation. However, a trend for comparatively more pronounced lesions can be observed in aged NHPs that were infected with SARS-CoV (**Figure 2**) (**Table 1**). Additionally, a notable difference lies in the tropism for nasal epithelium. Although results need confirmation in directly comparative experimental setups, no viral replication was detected in the nasal turbinates of NHPs infected with SARS-CoV, contrasting observations of SARS-CoV-2 infected NHPs (37).

2.2.3. Ferrets. Ferrets are a common model for respiratory infections and were therefore also frequently utilized for SARS-CoV and SARS-CoV-2 studies. However, after infection with SARS-CoV-2, they mimic only mild forms of disease, and the viral replication is mainly restricted to the upper respiratory tract (**Figure 2**) (**Table 1**).

In SARS-CoV-infected ferrets, lethargy, fever, sneezing, and even lethal outcomes were sporadically observed. Viral replication was found in trachea, lungs, and tracheobronchial lymph nodes, peaking at 5–6 dpi. Histologically, indications of mild alveolar damage, alveolar edema,

and perivascular and peribronchial lymphocytic infiltration, as well as lymphohistiocytic bronchopneumonia were observed. Pulmonary lesions involved up to 10% of the lung surface (25, 26, 35, 38).

Only mild symptoms of disease were observed in SARS-CoV-2-infected ferrets, including an elevation of body temperature, lethargy, nasal discharge, and coughing (27). Hematological alterations such as mild lymphopenia and neutrophilia have been described (29). Elevated inflammatory cytokines, including chemokine ligand 8 (CCL8), CXCL9, and CCL2, were observed. SARS-CoV-2 infection also generated a unique gene signature, characterized by an enrichment of genes associated with cell death and leukocyte activation, such as IL1A and CXCL8 (39). Viral replication could be found only in the upper respiratory tract, mainly in nasal turbinates, and no infectious virus was recovered from the lungs of infected animals (40). Peaks of viral replication appeared at 2 dpi and lasted until 14 dpi. Microscopically, bronchial submucosal granulomatous foci with eosinophilic material and collagen fragments were described. Furthermore, pulmonary perivasculitis and vasculitis, eosinophilic and histiocytic inflammation within alveolar spaces, and accumulation of cell debris along alveolar and bronchial epithelium were detected in the lower respiratory tract (41).

Similar to the comparison between SARS-CoV-2 and SARS-CoV in NHPs and hamsters, definitive conclusions cannot be drawn in ferrets due to limited and variable studies on SARS-CoV. However, a clear distinction can be found with SARS-CoV replicating and causing pathological changes in the lower respiratory tract of ferrets, whereas an infection with SARS-CoV-2 is limited to the upper respiratory tract and barely causes apparent disease. Furthermore, it is worth noting that a higher level of SARS-CoV-2 replication was observed in the nasal turbinates of infected animals.

3. TRANSMISSION MECHANISMS OF SARS-CoVs

3.1. Transmission in Humans

Both SARS-CoV and SARS-CoV-2 are airborne and transmitted via respiratory droplets generated by coughing and sneezing. During SARS-CoV infection, nasal viral shedding peaked at approximately day 10 after onset of symptoms (42, 43). In contrast, in nasal and throat swabs obtained in the beginning of the SARS-CoV-2 outbreak, the viral load peaked soon after symptom onset, with nose titers being higher than throat titers (44). These distinctions likely explain why SARS-CoV did not spread to the same global extent as observed with SARS-CoV-2 and why a pandemic of SARS-CoV could be prevented relatively soon by public health measures. Moreover, in a human challenge study of SARS-CoV-2, viral shedding from infected individuals into the environment was strongly correlated with viral titers in nasal swabs, indicating the nasal transmission route (45). In the nasal respiratory mucosa, SARS-CoV-2 targets ciliated cells (46). Because of the similar stability of SARS-CoV-2 (strain USA-WA1/2020, 614D) and SARS-CoV (strain Tor2) viral particles under experimental conditions (47), these observations raise questions on whether SARS-CoV-2 exhibits enhanced fitness in the nasal respiratory mucosa and whether this disparity contributes to its transmissibility. In addition to nasal respiratory mucosa, a postmortem study showed that in the olfactory mucosa, sustentacular cells were the main targets of SARS-CoV-2 infection but not olfactory sensory neurons. Nevertheless, the infected sustentacular cells may lead to transient olfactory dysfunction in COVID-19 patients, appearing as anosmia, one of the common symptoms of COVID-19 (46). Whether the infected sustentacular cells contribute to the viral transmission is unclear. Despite one reported case of SARS-CoV-infection-related anosmia (48), there is no published study about the susceptibility of olfactory sensory neurons or sustentacular cells to SARS-CoV infection.

3.2. Transmission in Animal Models

Animal models enable a controlled experimental setting to investigate the dynamics of viral transmission, providing insights into the routes and mechanisms by which the virus spreads, as well as the viral shedding patterns.

In ferrets, SARS-CoV was successfully isolated from pharyngeal swabs of infected animals and was efficiently transmitted to cohoused animals (25). Interestingly, no virus was detected in nasal swabs in this study, which stands in sharp contrast to the shedding pattern of SARS-CoV-2 in ferrets. The kinetics of viral shedding differed between donor and recipient animals, with a later peak of shedding in recipient animals, mimicking delayed viral shedding after onset of clinical manifestation as described in SARS-CoV infection in humans (38). SARS-CoV-2-infected ferrets transmitted virus efficiently via direct contact and by air. The shedding pattern of the virus in donor and direct/indirect recipient animals was comparable (49).

A comprehensive study on the comparative transmission of SARS-CoV and SARS-CoV-2 in ferrets reported that both viruses maintained their infectivity over distances exceeding 1 m through the air. Transmission to recipient animals was observed for both viruses, with SARS-CoV showing slightly higher efficiency (50). Contrary to findings by Martina et al. (38), the shedding kinetics were similar between recipients and donors, as well as between the two viruses. Viral RNA was detected in throat and nose swabs, with slightly higher levels in throat swabs. SARS-CoV was transmitted much faster in ferrets as compared with humans, likely due to the constant exposure of recipients to unidirectional airflow, optimizing their exposure. This factor may contribute to the high transmission efficiency observed (50). It is also noteworthy that advanced age was associated with enhanced viral shedding in SARS-CoV-2-infected-ferrets (51). Furthermore, SARS-CoV-2 lacking the S1/S2 furin cleavage site was shed to lower titers from infected ferrets and failed to transmit to cohoused sentinel animals, underlying the importance of the furin cleavage site for SARS-CoV-2 transmission (52). SARS-CoV-2-infected hamsters also transmitted virus effectively through direct contact and by air, whereas fomite transmission was not efficient (53, 54). In NHPs, infectious SARS-CoV was detected in nasal and throat swabs (37, 40), while SARS-CoV-2 shedding was detected in respiratory and rectal samples, with the highest viral titers in nose swabs (29, 30). The kinetics of SARS-CoV shedding in NHPs were comparable to those of SARS-CoV-2 (37, 55).

Despite conflicting data, no major differences in kinetics and amplitude of shedding in animal models can be defined for SARS-CoV and SARS-CoV-2. However, indications for a reduced nasal shedding were occasionally reported in SARS-CoV-infected-ferrets and NHPs, but this aspect has not been extensively investigated in hamsters.

4. PATHOGENESIS MECHANISMS OF SARS-CoVs

Understanding the pathogenesis of SARS-CoV and SARS-CoV-2 involves elucidating the factors that initiate the inflammatory cascade resulting in ARDS. The viruses can cause lung damage directly by the infection and destruction of the alveolar epithelial cells or indirectly by induction of immune mediators (6, 56). Severe SARS-CoV infection and COVID-19 are associated with hypercytokinemia (i.e., the cytokine storm), which can cause life-threatening complications, such as viral sepsis and multiorgan failure (57, 58). A comprehensive understanding of the pathogenesis of SARS-CoVs requires combining the analysis from clinical human samples, animal models, and in vitro models.

4.1. Pathogenesis in the Human Respiratory Tract

The alveoli are constructed with thin AT1 cells, which are responsible for gas exchange, and cuboidal AT2 cells that are the progenitors for AT1 cells during lung regeneration (59). AT2 cell

hyperplasia has been observed in the lungs of fatal cases of both SARS-CoV and SARS-CoV-2 infections (21–23, 60). In COVID-19 lungs, scRNA-seq revealed that both AT1 and AT2 cells expressed lower levels of cell-type identification markers but elevated expression of genes involved in apoptosis. Furthermore, AT2 cells lost the ability to differentiate toward AT1 cells, displaying an inflammation-associated transient progenitor cell state, impairing lung regeneration (61, 62). This is in line with observations in SARS-CoV fatal cases by Chen et al. (63), where viral positive lung cells belonged to a novel subset exhibiting stem/progenitor status, missing AT1 and AT2 markers. Additionally, in lung autopsies from SARS-CoV infection, viral-infected $ACE2^+$ cells produced a higher level of proinflammatory cytokines (64). Further investigation is needed to determine whether this unique subset of SARS-CoV-positive lung cells underwent a similar inflammatory state as observed in SARS-CoV-2 infection and whether it contributed to the disease progression during SARS-CoV infection.

Another important observation in lungs of COVID-19 patients is the prevalence of syncytia. These syncytia in the postmortem tissues not only were positive for SARS-CoV-2 spike protein but also contained CD45-positive cells, suggesting that syncytia tend to internalize lymphocytes (65). Although the presence of syncytia has also been observed in the lungs of SARS-CoV patients, it is noteworthy that SARS-CoV does not exhibit high fusogenicity in in vitro human airway models. The precise mechanism underlying the formation of syncytia in SARS-CoV infection remains uncertain.

While type I IFNs (IFNα and IFNβ) are widely expressed along the respiratory tract, and can lead to immunopathology during infection, type III IFN (IFNλ) responses are primarily restricted to mucosal surfaces and provide antiviral protection without adverse proinflammatory responses. Factors such as timing and duration of immune responses may contribute to the disease progression. ScRNA-seq of cells obtained from nasopharyngeal swabs of severe COVID-19 patients revealed moderate induction of type I or type II IFN–responsive genes in viral-infected ciliated cells. Moreover, elevated levels of inflammatory cytokines as well as type I and III IFNs were detected in the bronchoalveolar lavage fluid from severe COVID-19 cases, but not in nasopharyngeal swabs, suggesting that the possible cause of severe disease was due to unrestricted viral replication in the upper airway and tissue damage in the lower airway (66, 67). In the context of SARS-CoV infection, however, studies are available only for the systemic level of type I and III IFNs. During the acute phase in severe and nonsevere patients, type I and III IFNs, as well as related chemokines such as CXCL10, were upregulated in the peripheral blood. As the disease progressed, self-sustaining expression of proinflammatory chemokines and interferon-stimulated genes (ISGs), accompanied with deficient antigen presentation genes, led to poor disease outcome (57, 68).

Lung tissue injury and inflammation attracts immune cells. ScRNA-seq on lungs of lethal COVID-19 cases thus revealed a dense presence of abnormally activated monocyte-derived macrophages and alveolar macrophages, characterized by an increase of proinflammatory macrophages and a decrease of anti-inflammatory macrophages (61, 62). There was no significant increase in T cell populations observed in COVID-19-affected lungs, and only a modest upregulation of cytokines and programs associated with T cell activation and tissue residency, indicating impaired T cell responses. Notably, monocyte/macrophage-derived IL1β and epithelial cell–derived IL6 were identified as distinct characteristics of SARS-CoV-2 infection (61). In the lungs of SARS-CoV fatal cases, macrophages, both infected and uninfected, were identified (20, 21). Furthermore, SARS-CoV-infected T cells were detected in SARS-CoV lung autopsies in one study. It was hypothesized that these infected T cells played a role in lymphopenia and facilitated viral dissemination to other organs (21). However, the specific function of these SARS-CoV-infected immune cells was not extensively investigated in the patient samples. **Figure 3**

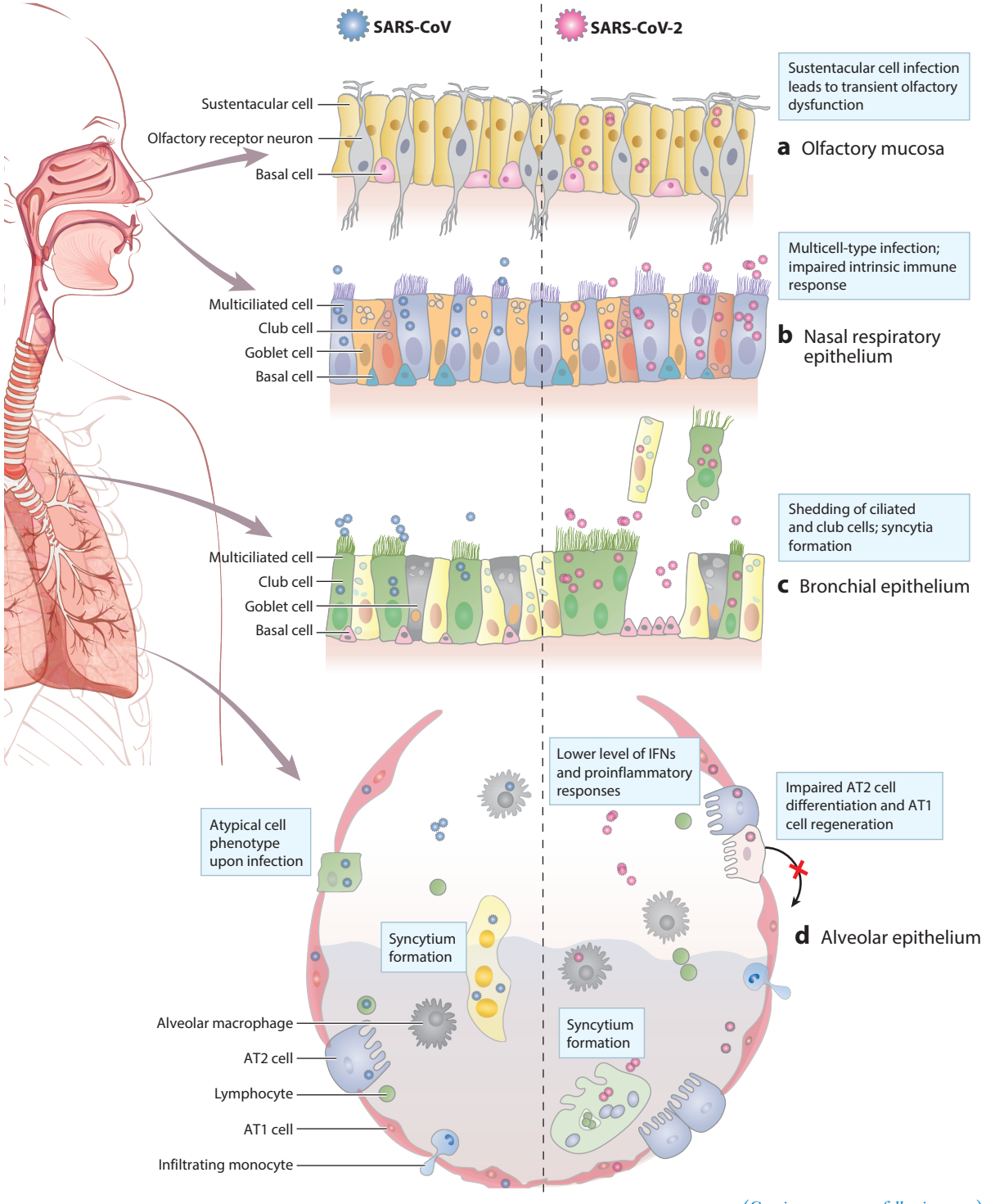

(*Caption appears on following page*)

Figure 3 (*Figure appears on preceding page*)

Comparative pathogenesis of SARS-CoV and SARS-CoV-2 in the human respiratory tract. (*a*) SARS-CoV-2 infects sustentacular cells in the olfactory mucosa, causing transient olfactory dysfunction such as anosmia in some patients. It remains unclear whether SARS-CoV infects the olfactory mucosa. (*b*) In the nasal respiratory epithelium, SARS-CoV infects ACE2-expressing ciliated cells. In contrast, SARS-CoV-2 efficiently infects both ciliated cells and goblet cells, leading to uncontrolled viral replication due to weak intrinsic immune responses in the nose. (*c*) In the lower conductive airway, SARS-CoV-2 infection results in the shedding of infected cells and triggers epithelial regeneration. It also promotes the formation of syncytia, facilitating virus spread. There is limited knowledge regarding SARS-CoV infection in the lower conductive airway, except that it infects ACE2-positive ciliated cells. (*d*) Both viruses can cause severe lung damage. SARS-CoV infection in the alveolar epithelium leads to the presence of a unique infected cell cluster and syncytia, although the fate of these cells remains unexplored. SARS-CoV-2 infection generally induces weaker IFNs and proinflammatory responses in the lungs, but in severe cases, inflammatory responses are elevated. Infected AT2 cells lose their ability to differentiate, impairing lung repair. There is formation of syncytia, which may contain lymphocytes. Abbreviations: AT1/AT2, alveolar type I/II pneumocyte; ACE2, angiotensin-converting enzyme 2; IFN, interferon; SARS-CoV, severe acute respiratory syndrome coronavirus. Figure contains elements adapted with standard license from **http://stock.adobe.com**.

summarizes the characteristics of SARS-CoV and SARS-CoV-2 pathogenesis in the human respiratory tract.

Innovative techniques such as single-cell omics have provided valuable opportunities to investigate the pathogenesis and immune response in SARS-CoV-2 infection (61, 62). During the initial outbreak of SARS-CoV in the early 2000s, the availability and development of innovative techniques such as single-cell omics were limited compared with the present day. Consequently, most studies on SARS-CoV were conducted using technologies that were available two decades ago. Even now, the feasibility of using suitable historical patient samples for high-resolution single-cell analysis remains a challenge in SARS-CoV studies. The advancements in in vivo and in vitro models present valuable opportunities to bridge the gaps in our understanding of SARS-CoV pathogenesis and facilitate comparative investigations with SARS-CoV-2, utilizing cutting-edge techniques. These approaches can provide important insights into the similarities and differences between the two viruses and enhance our understanding of their respective disease mechanisms.

4.2. Pathogenesis in Animal Models

In animal models, the severity and clinical outcomes of the diseases caused by SARS-CoV and SARS-CoV-2 are influenced by both host and viral factors. While host factors encompass a range of protective reactions, such as immune responses or cell death, they can also lead to enhanced disease when excessive or interfering with normal physiological functions, such as gas exchange in the lungs. On the other hand, viral factors are usually intrinsic properties that suppress a host response and enhance viral replication and dissemination. In contrast to in vitro platforms, animal models provide the physiological environments that encompass intricate cellular interaction and genetic modification, making them particularly valuable for the identification of systematic determinants of disease severity during SARS-CoV and SARS-CoV-2 infections.

4.2.1. Host factors. Immunosuppression experiments using animal models have highlighted the importance of an intact immune response in the context of SARS-CoV and SARS-CoV-2 infections. Hamsters treated with cyclophosphamide, which induced immunosuppression, showed more severe and prolonged disease, along with an expanded tissue tropism for both SARS-CoV and SARS-CoV-2 (69, 70). Depletion of $CD4^+$ T cells in BALB/c mice resulted in delayed clearance of SARS-CoV from the lungs, while $CD8^+$ T cell response was critical to protect C57BL/6 mice from lethal SARS-CoV outcomes. Additionally, a dysregulated proinflammatory signature of circulating T cells at baseline was associated with severe disease in mice with SARS-CoV infection (71). RAG2 knockout hamsters, lacking mature T and B cells, showed uniformly lethal outcomes following SARS-CoV-2 infection (70).

In vivo experiments have provided evidence that the pulmonary pathology observed in SARS-CoV and SARS-CoV-2 infections is primarily driven by immunopathology rather than the direct effects of viral replication. Supporting the role of immunopathology in SARS-CoV-2-induced lung damage, pulmonary pathology was significantly reduced in STAT2-knockout hamsters, along with increased viral loads and viral RNA dissemination in peripheral tissues (72). Different from humans, in hamsters, a proinflammatory expression profile, characterized by productive rather than dysregulated inflammation and a tendency toward T cell recruiting chemokines, was observed, which may explain the transient and self-limiting nature of SARS-CoV-2 infections in these animals (73). Furthermore, the critical role of Toll-like receptor signaling in controlling pulmonary pathology caused by SARS-CoV and SARS-CoV-2 has been repeatedly demonstrated (74, 75). Activation of nuclear factor kappa B (NF-κB) has also been identified as an important determinant of disease severity in mice and NHPs infected with SARS-CoV and SARS-CoV-2 (76–78).

Both SARS-CoV and SARS-CoV-2 infections in animals have shown a correlation between an increase of age and more severe disease, higher viral replication and shedding, and reduced viral clearance (31, 35, 79–81). Similar to the observations in humans (82), higher transcription levels of essential viral entry factors ACE2 and TMPRSS2 (transmembrane serine protease 2) were detected in the respiratory tract of aged ferrets and mice, suggesting that hosts with advanced age might be more susceptible to infections (83). Furthermore, an age-related increase in immune response and the presence of a proinflammatory microenvironment with an accumulation of $CXCR3^+$ (C-X-C motif chemokine receptor 3) cells in the lungs have been observed in SARS-CoV-2-infected NHPs and mice (51, 77, 84, 85), suggesting that age-related factors play a significant role in the pathology of CoV infections. Besides, sex is an important determinant for the disease outcome after infection with both SARS-CoV and SARS-CoV-2. Multiple experiments indicate that more severe disease, as well as enhanced viral replication and immunopathology, was observed in male animals (86–88).

Coagulative disorders have been identified as an important factor for both SARS-CoV and SARS-CoV-2 disease severity. In mouse models, elevated levels of profibrotic cytokine transcripts and fibrin deposition in the lungs were observed during lethal SARS-CoV infections (89). Similarly, evidence of coagulation dysfunction was identified in SARS-CoV-2-infected NHPs (90), accompanied by the upregulation of pathways associated with complement and platelet activation, thrombosis, vascular injury and repair, and neutrophil degranulation (31). Additionally, both SARS-CoV-2-infected mice and NHPs displayed endothelial activation and dysfunction in pulmonary vessels, characterized by adhesion of platelets and immune cells (91). Proteomic analysis of the lung tissues from SARS-CoV-2-infected hamsters further revealed the activation of complement cascade, coagulation cascade, platelet activation, ferroptosis, and focal adhesion (92).

SARS-CoV infection and the spike protein itself reduced ACE2 expression, which was an additional pathogenic factor. The renin-angiotensin system has a crucial role in severe acute lung injury, and ACE2 is critical in acute lung failure (93). Similarly, downregulation of ACE2 was observed in SARS-CoV-2-infected hamsters (94). Although the sequences of hamster and human ACE2 are relatively similar, slight differences at position 82 were hypothesized to be responsible for the absence of fatal disease following infection with SARS-CoV and SARS-CoV-2 in hamsters (40). However, it was assumed that susceptibility to infection was multifactorial, influenced not only by genetic ACE2 composition but also by organ-specific ACE2 expression, additional receptors/proteases, and host immune responses (95).

4.2.2. Viral factors. SARS-CoVs contain several open reading frames (ORFs) in their genomes, generating different viral proteins. The viral proteins and genetic variations of SARS-CoVs

that contribute to viral replication and immune evasion have the potential to influence their pathogenicity. The envelope (E) protein of SARS-CoV was identified as an important virulence factor in mice and hamsters. A deletion of the SARS-CoV E gene led to reduced lung injury with limited neutrophil influx and increased presence of $CD4^+$ and $CD8^+$ T cells. The E protein PDZ-binding motif (PBM), a domain involved in protein–protein interactions, and the E protein ion channel activity were major determinants of virulence (76, 96, 97). In mice, the PBM of SARS-CoV and SARS-CoV-2 E proteins were involved in dysregulating gene expression related to ion transport and cell homeostasis (98). Additionally, the SARS-CoV-2 E protein alone was able to cause ARDS-like damages in mice (99). The SARS-CoV strain Frankfurt-1 possesses a unique 45-nucleotide deletion in its ORF7b protein. Hamsters inoculated with a virus carrying this deletion showed an increased viral burden in their lungs. The presence of intact ORF7b was mainly found in early variants of SARS-CoV, suggesting its potential role in limiting the spread of SARS during the initial phase of the epidemic (100). Infection of K18-ACE2 mice with recombinant SARS-CoV-2 variants identified ORF3a and ORF6 as the major contributors of viral pathogenicity, with ORF6 as a potent inhibitor of the host innate immune response and ORF3a inducing cytokines being favorable for viral replication and tissue damage (101). Furthermore, SARS-CoV-2 ORF8 was identified as an important virulence factor, and its deletion attenuated pulmonary inflammation in hamsters (78).

4.3. Pathogenesis in In Vitro Studies: Cellular Entry Mechanism

Both SARS-CoV and SARS-CoV-2 exploit ACE2 as the cellular receptor for host entry (102, 103). In silico and in vitro investigations have yielded comprehensive insights into the interaction of the spike proteins of SARS-CoV and SARS-CoV-2 with the human ACE2 receptor and cellular proteases, shedding light on the distinct mechanisms employed by these two human coronaviruses to facilitate their cellular entry. In vitro studies often use cell lines expressing the ACE2 receptor and/or the proteases, together with pseudoviruses that were engineered to express the viral spike proteins. However, it is important to acknowledge that cell lines and pseudoviruses have limitations in representing the complexity of the human respiratory system and authentic viral infection and may cause false conclusions (104, 105). Therefore, it is crucial to complement these studies with physiologically relevant models such as primary cultures, human organoids, and in vivo experiments to obtain a comprehensive understanding of the viral entry mechanism.

Additionally, choice of spike variants is crucial for comparative investigations of SARS-CoV and SARS-CoV-2 entry mechanisms. The D614G mutation in the spike protein of SARS-CoV-2, which emerged in March–May 2020, led to enhanced binding to the ACE2 receptor and viral particle stability. This variant played a significant role in the early stages of the pandemic and is commonly used for comparative studies with SARS-CoV in in vitro investigations (106).

Following successful receptor binding, SARS-CoV undergoes two proteolytic cleavage events that lead to the activation and conformational change of spike proteins, priming the viral cell entry machinery. The first cleavage occurs at the S1/S2 junction, whereas the second cleavage site is adjacent to the S2′ site within the S2 subunit. The second cleavage exposes the fusion peptide, which triggers fusion of viral and cellular lipid bilayers, facilitating the release of the viral ribonucleoprotein complex into the host cell. In the case of SARS-CoV-2, the first cleavage at the S1/S2 junction occurs during viral production, requiring only the second cleavage of the spike protein on the target cells after the receptor binding (10). For both SARS-CoV and SARS-CoV-2, as observed in cell lines, TMPRSS2 mediates plasma membrane fusion entry, while cathepsin L (CTSL) regulates endolysosome-mediated entry (10, 11).

The utilization of specific receptors and proteases by SARS-CoV and SARS-CoV-2 significantly impacts their cellular and tissue tropism, representing a critical factor in viral transmission

and pathogenesis. For example, the cell entry mechanism of SARS-CoV-2 on human nasal epithelial cells has been well studied using a primary nasal epithelium model (12, 13). The SARS-CoV-2 virions (614G variant) firstly attached to motile cilia via the ACE2 receptor. The virus then traveled to the cell body through ciliary trafficking. Viral replication in these cells triggered the formation of apically extended and highly branched microvilli, which facilitated virus egress. The highly infectious omicron variant of SARS-CoV-2 displayed a higher binding affinity to motile cilia and a faster viral entry compared with the ancestral strain, suggesting a mechanism of the rapid spread observed in the community (13). A comparative analysis of the entry machinery of SARS-CoV and SARS-CoV-2 in such in vitro human nasal epithelium systems would be valuable to gain insights into their respective transmissibility.

4.3.1. Tissue/cell expression of ACE2 and proteases. Considering that viral entry of SARS-CoV and SARS-CoV-2 is a multifactorial-dependent procedure, efforts have been made to understand the coexpression profile of cellular viral entry factors in human tissues.

In the human nasal airway, nasal goblet cells and multiciliated cells compose the highest fraction of $ACE2^{+}TMPRSS2^{+}$ cells (107), matching the fact that these cells are the main targets of SARS-CoV-2 in the human nose. In the olfactory mucosa, ACE2 and TMPRSS2 are coexpressed in sustentacular and basal cells but not in olfactory sensory neurons (108). This is consistent with the observation that SARS-CoV-2 infects sustentacular cells but not olfactory sensory neurons in postmortem samples (46). CTSL, which has been observed to be recruited by both SARS-CoV and SARS-CoV-2 in cell lines, is coexpressed with ACE2 in olfactory mucosa and pericytes in lung (109). In the lower lung, ACE2 and TMPRSS2 mRNA are coexpressed in AT1 and AT2 cells. It is worth noting that TMPRSS2 is expressed only in a subset of ACE2-positive cells, indicating that other alternatives can be recruited by the viruses (107). As examined in lung, nasal, and gut epithelial cells, the coexpression of TMPRSS2 and ACE2 is associated with expression of key immunological genes and genes involved in viral infection, indicating the possible trigger of responses such as cytokine storm during disease development (109). Furin mRNA is expressed in a wide range of human tissues, including its high expression in $ACE2^{+}/TMPRSS2^{+}$ nasal ciliated cells and AT2 cells (110, 111). Since SARS-CoV-2 utilizes furin but SARS-CoV does not, the abundance of furin may contribute to the tissue tropism and replication kinetics of SARS-CoV-2.

4.3.2. Interaction of spike proteins with the receptor/proteases. Similar to the SARS-CoV spike protein, the SARS-CoV-2 spike protein interacts with the cellular receptor through a receptor-binding domain (RBD), which contains a core and a receptor-binding motif (RBM) (112, 113). Both spike proteins have a similar number of hydrogen bonds and salt bridges at the RBMs. Although structurally very similar, compared with the SARS-CoV RBM, the SARS-CoV-2 RBM forms a bigger binding interface, which provides more contact with ACE2. The enhancement in receptor interaction is probably caused by structural changes in the ACE2-binding ridge by four residues (482–485 GVEG), and at L455, F486, Q493, and N501 (112, 113). Binding kinetics assays further confirmed a higher binding affinity to ACE2 of the SARS-CoV-2 RBD than that of the SARS-CoV RBD (112–114) (**Figure 4**).

The seasonal alphacoronavirus NL63 also uses ACE2 for cellular entry. Comparing the utilization of ACE2 between low-pathogenic NL63 and the high-pathogenic SARS-CoVs is informative for factors influencing disease severity. The spike of NL63 has less interface surface area with ACE2 compared with those of SARS-CoV and SARS-CoV-2 (115). Each virus uses specific segments at the spike–ACE2 interface. Evaluation of the interaction energy between ACE2 and viral spike proteins revealed the binding affinity order of the three coronaviruses as SARS-CoV-2 > SARS-CoV > NL63 (116). Nevertheless, the binding affinity to the receptor cannot solely explain all differences observed during infection.

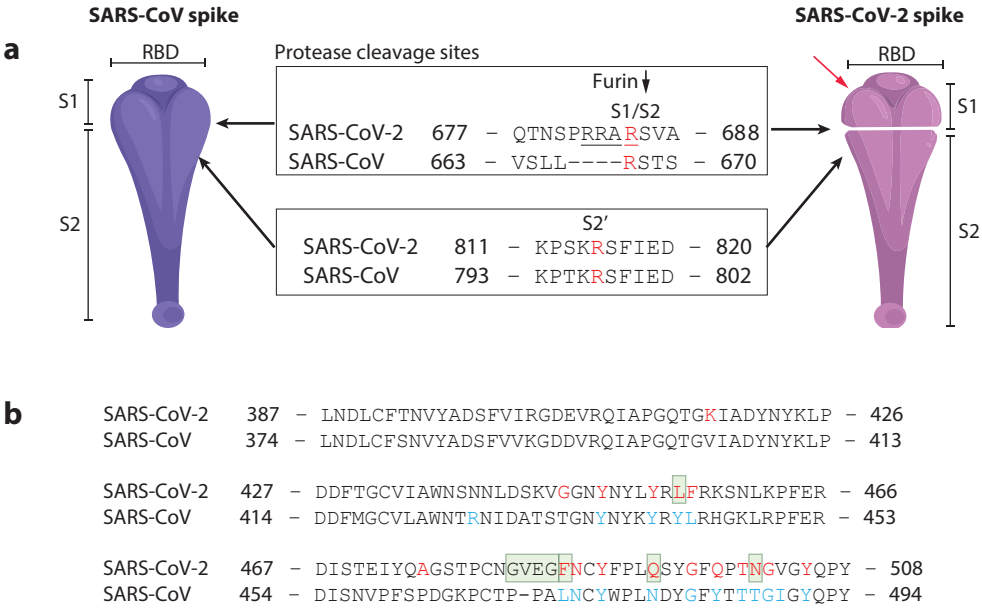

Figure 4

Differences in receptor and protease usage by spikes of SARS-CoV and SARS-CoV-2. (*a*) The protease cleavage sites on the spikes of SARS-CoV and SARS-CoV-2, with the arginine cleavage site indicated in red letters. The presence of a furin-cleavable multibasic cleavage site (residues *underlined*) at the S1/S2 junction of the SARS-CoV-2 spike protein distinguishes it from the SARS-CoV spike protein. Additionally, the SARS-CoV-2 spike protein contains an extra cleavage site for TMPRSS2 in the RBD region (*red arrow*). (*b*) The two spike proteins interact with ACE2 via structurally similar RBMs. Contacting residues in the SARS-CoV-2 RBM and SARS-CoV RBM are indicated by red letters and blue letters, respectively. However, the SARS-CoV-2 spike protein exhibits a larger and stronger binding interface with ACE2 due to specific critical residues, highlighted in green boxes. Abbreviations: ACE2, angiotensin-converting enzyme 2; R, arginine; RBD, receptor-binding domain; RBM, receptor-binding motif; SARS-CoV, severe acute respiratory syndrome coronavirus; TMPRSS2, transmembrane serine protease 2. Sequences used for this figure are obtained from SARS-CoV strain HKU39849 and SARS-CoV-2 strain Germany/BavPat1/2020 on the basis of published data (112, 113). Figure contains elements adapted with standard license from **http://stock.adobe.com**.

The adaptation of a coronavirus to human cells is reflected by its receptor binding—a phenomenon that was already observed during the outbreak of SARS-CoV. The spike protein of SARS-CoV strain Tor2, obtained from the earlier outbreak period, showed strong binding to human ACE2, while the spike proteins from a strain that emerged later during the outbreak (strain GD) and from a SARS-CoV-like virus (SZ3) exhibited efficient binding to palm civet ACE2 but less binding to human ACE2. Residues 487 and 479 on the spike proteins were found to be crucial for association with the human receptor. This finding supported the hypothesis that the late outbreak was caused by a newly introduced viral strain that had yet to fully adapt to the human host, resulting in decreased transmissibility (117).

Following receptor binding, the spike protein of SARS-CoV undergoes a crucial first cleavage at the S1/S2 site by TMPRSS2, which is a prerequisite for subsequent cleavage at the S2′ site. Unlike SARS-CoV, the S1/S2 junction of the SARS-CoV-2 spike protein contains a distinctive multibasic cleavage site (MBCS) with three basic arginines interrupted by a nonpolar alanine (RRAR). This MBCS can be *cis*-cleaved by the ubiquitous cellular protease furin (**Figure 4**).

This unique MBCS motif on SARS-CoV-2 facilitates a faster serine protease-mediated entry on Calu-3 cells (118). A mutant SARS-CoV-2 that lacked the MBCS motif had impaired replication in Calu-3 cells (119). This aligns with in vivo observations that SARS-CoV-2 with MBCS deficiency showed less transmission in ferrets (52). These data highlight the significance of this motif for efficient viral replication and spreading in respiratory epithelium.

Both SARS-CoV and SARS-CoV-2 can utilize TMPRSS2 for the second proteolytic cleavage step. In the case of the SARS-CoV spike protein, TMPRSS2 cleaves at the R797 site before the fusion peptide (120), whereas in the SARS-CoV-2 spike protein, TMPRSS2 can efficiently cleave the C-terminus of the RBD, in addition to upstream of the fusion peptide in S2 (121) (**Figure 4**). The furin usage by SARS-CoV-2 reduces the reliance on proteolytic events occurring on the target cell surface, unlike SARS-CoV, which necessitates two cleavage steps mediated by TMPRSS2. The presence of the MBCS and the utilization of furin likely contribute to the enhanced and rapid spread of SARS-CoV-2 within the human airway epithelium (**Figures 4** and **5**).

This difference in using furin further affects the entry routes used by these two viruses in cell lines. SARS-CoV-2 pseudovirus (614D) cell entry depended more on TMPRSS2 expression than SARS-CoV pseudovirus in $293T^{ACE2+}$ cells. But a SARS-CoV-2 mutant with a deficient furin cleavage site no longer heavily depended on TMPRSS2 (122). SARS-CoV, which generally requires more proteolytic activation of sufficient numbers of spike proteins on the target cells, was able to utilize CTSL-mediated entry more efficiently when TMPRSS2 was absent. It was hypothesized that the furin cleavage resulted in an unstable status of the SARS-CoV-2 spike, which was further destabilized in the acidifying endosome, impairing the endocytic entry route mediated by CTSL. The 614G variant of the SARS-CoV-2 spike protein, known for its increased stability, had reduced susceptibility to the effects of TMPRSS2 (122). This impact of the furin cleavage site was further demonstrated in clinical isolates of SARS-CoV-2 (614G) propagated in VeroE6 cells. These viruses obtained mutations in the MBCS, causing adaptation to the CTSL-mediated entry pathway present in VeroE6 cells (105) (**Figure 5**). These observations undoubtedly demand further validation using more relevant cell models, rather than cell lines.

Furthermore, the presence of the MBCS in the SARS-CoV-2 spike protein resulted in a stronger fusogenicity compared with SARS-CoV in human airway organoid-derived air-liquid interface (ALI) cultures, potentially facilitated by furin utilization (118). Apart from furin, the process of SARS-CoV-2-mediated cell–cell fusion also involves TMPRSS2, which enhanced the fusion process by proteolytically processing both the SARS-CoV-2 spike and ACE2 receptor in cell lines (123) (**Figure 5**). The enhanced cell–cell fusion of SARS-CoV-2 may hold significant implications for the pathogenesis, as SARS-CoV-2 potentially can spread efficiently through syncytia formation in the human airway (124). Notably, there is a lack of quantitative evidence comparing the extent of syncytia formation caused by SARS-CoV and SARS-CoV-2 infection in both patient and experimental animal lungs.

In addition to TMPRSS2, there are other serine proteases that are expressed in the human respiratory tract and have the ability to cleave spikes from SARS-CoV and SARS-CoV-2. These serine proteases include TMPRSS11A, TMPRSS11D, TMPRSS11E, and TMPRSS13 (125, 126). The ability of both SARS-CoV and SARS-CoV-2 to exploit various serine proteases expressed in the human respiratory tract to facilitate viral entry provides a higher degree of adaptability and thus contributes to the intricate cellular and tissue tropism observed in clinical settings.

4.4. Pathogenesis in In Vitro Studies: Tissue Tropism and Innate Immune Responses

Compared with experimental animals, in vitro models provide a controlled and focused approach to studying specific cellular or molecular events associated with SARS-CoV and SARS-CoV-2

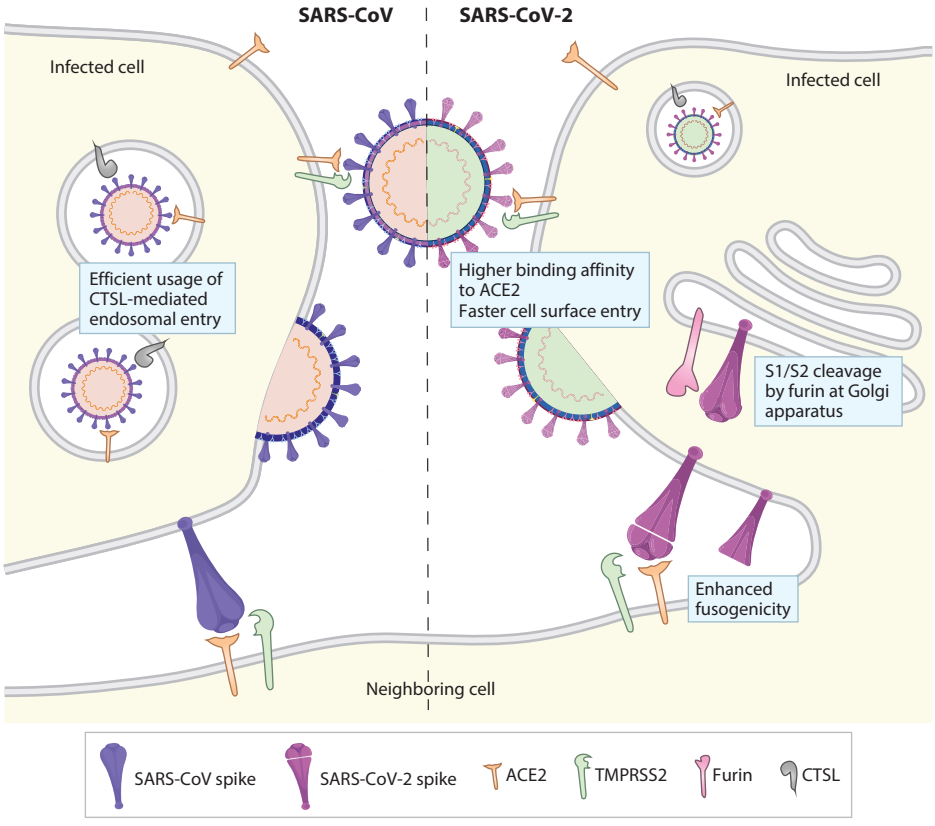

Figure 5

In vitro observations on cellular entry by SARS-CoV and SARS-CoV-2. During viral entry, the SARS-CoV-2 spike protein shows a higher affinity for ACE2. The presence of an MBCS enables SARS-CoV-2 to enter cells more rapidly through the membrane fusion pathway. In contrast, SARS-CoV can utilize both membrane fusion and CTSL-mediated endosomal entry pathways. Furin cleavage of the newly synthesized SARS-CoV-2 spike protein in the Golgi apparatus enhances its ability to efficiently bind to ACE2 and utilize TMPRSS2, thereby contributing to its stronger fusogenicity and viral spread. Abbreviations: ACE2, angiotensin-converting enzyme 2; CTSL, cathepsin L; MBCS, multibasic cleavage site; SARS-CoV, severe acute respiratory syndrome coronavirus; TMPRSS2, transmembrane serine protease 2. Figure contains elements adapted with standard license from **http://stock.adobe.com**.

pathogenesis. Various in vitro models, such as those based on postmortem patient samples, ex vivo tissue explants, and cell lines expressing key receptors and proteases, have been used to investigate viral entry, cellular tropism, and innate immune responses. While cell line models offer a high-throughput system to explore viral–host interaction networks for these viruses (127, 128), they lack the physiological context of viral infection and may induce undesired viral adaptations (104, 105). In contrast, in vitro human primary airway cultures resemble the morphological and physiological features of the human conducting airways more closely and have been instrumental in studying infection kinetics and cellular tropism for both SARS-CoV and SARS-CoV-2 (12–14). Organoid models derived from stem cells offer regeneratable and self-organized cells that exhibit functional and architectural characteristics of the corresponding tissues. Human pluripotent stem cell–derived and multipotent adult stem cell–derived respiratory organoids, representing fetal/neonatal and mature states, respectively, have been extensively utilized to study SARS-CoV-2

infection kinetics, entry mechanisms, and immune responses (105, 129–131). Notably, the use of these organoid models to study SARS-CoV is still limited.

Furthermore, selecting appropriate viral strains is crucial for comparative investigations of SARS-CoV and SARS-CoV-2 pathogenesis. The SARS-CoV-2 variant with D614G mutation in the spike protein has shown increased replication and transmissibility in various cultures and animal models (106) and is widely used in in vitro studies. In the case of SARS-CoV, a gradual deletion occurred in the ORF8 coding sequence during the epidemic. This deletion was present in all strains involved in the middle and late phases of the epidemic and resulted in attenuated replication in cell lines (132). Therefore, caution must be exercised when comparing the replication of this ORF8-deleted variant of SARS-CoV with SARS-CoV-2 (133).

4.4.1. Observations in upper airway models. In humans, SARS-CoV exhibits a peak in shedding approximately 10 days after symptoms appear, whereas SARS-CoV-2 shows a peak shortly after symptom onset (6, 42, 43). Besides, in vivo investigations indicated a higher replication of SARS-CoV-2 compared with SARS-CoV in the nose. It is therefore crucial to investigate whether SARS-CoV-2 displays enhanced replication or fitness in the human nasal mucosa and whether this disparity contributes to its transmissibility.

Several studies that applied scRNA-seq on nasopharyngeal swabs of COVID-19 patients have revealed that in the nasal mucosa, SARS-CoV-2 mainly targets $ACE2^{+}TMPRSS2^{+}$ ciliated cells and goblet cells (66, 134). In contrast, there is limited literature on nasal cellular tropism of SARS-CoV in patients, except for a few in vitro studies showing that SARS-CoV infected $ACE2^{+}$ ciliated nasal epithelial cells in culture (14, 15).

Considering the lower pH (approximately 6.3) in the nasal cavity compared with the neutral pH (approximately 7.5) in the lumen of the human lungs, the pH level may contribute to the stability and infectivity of the viruses. In $293T^{ACE2+TMPRSS2+}$ cells, the SARS-CoV spike-carrying pseudoviruses exhibited higher infectivity at pH 7.5 than at pH 6.3. Conversely, the SARS-CoV-2 pseudoviruses (both 614D and 614G) showed a preference for lower pH conditions (125).

Impaired intrinsic immune responses in the nose were observed in patients with severe COVID-19. ScRNA-seq of cells obtained from nasopharyngeal swabs of patients with severe COVID-19 revealed absence of antiviral responses in viral infected cells, suggesting the possible pathogenesis of severe disease by enhanced viral replication in the upper airway (66). Furthermore, when infecting human primary nasal epithelial cultures with SARS-CoV-2 (614D strains), a delayed induction of type I and III IFNs and IFN-regulated gene expression relative to viral gene replication was observed at 1 dpi (135, 136).

4.4.2. Observations in lower conducting airway models. Investigation on postmortem samples from SARS-CoV infection detected viral antigens in ciliated epithelial cells lining bronchioles, bronchi, and trachea using detection methods such as electron microscopy, IHC, and in situ hybridization (21, 60). The primary human tracheobronchial culture model confirmed that SARS-CoV primarily infected ACE2-expressing ciliated cells (15, 137). In the fatal cases of COVID-19, viral antigens were detected in ciliated cells in trachea, bronchi, and bronchioles by IHC (22, 23). Close examination of tracheal tissue obtained from deceased COVID-19 patients revealed significant tissue damage. The infection led to the shedding of ciliated and club cells into the lumen, leaving the underlying basal cells exposed, and was accompanied by extensive cell proliferation (138) (**Figure 3**).

The establishment of in vitro human airway models enabled the comparative investigations for SARS-CoV and SARS-CoV-2. In human airway organoid-derived ALI cultures, SARS-CoV-2 (strain Germany/BavPat1/2020, 614G) infection resulted in the formation of syncytia, characterized by the fusion of multiple uninuclear cells. In contrast, such syncytia formation was not

observed in the human airway ALI culture upon SARS-CoV (strain HKU39849) infection. This distinction may be attributed to the presence of an MBCS at the S1/S2 junction of the spike protein of SARS-CoV-2. The increased fusogenicity of SARS-CoV-2 on human airway epithelium is a plausible strategy to evade extracellular immune surveillance and enhance viral dissemination. Consequently, this enhanced fusogenicity likely contributes to the transmission and pathogenesis of SARS-CoV-2 (118, 124), similar to what has been observed in a ferret model (52). Notably, syncytia were observed in lungs of SARS-CoV-infected patients and NHPs (20, 21, 25). It is possible that these observed syncytia had originated from macrophages upon SARS-CoV infection. As a result, the evidence regarding the syncytia formation of SARS-CoV in human airway ALI culture, where professional immune cells including macrophages are absent, remains inconclusive.

Given that a temperature gradient exists in the human respiratory tract, with mucosal temperature higher in the lower respiratory tract, temperature sensitivity was examined for SARS-CoV and SARS-CoV-2. In primary human tracheobronchial epithelial cells, SARS-CoV-2 (strain München-1.1/2020/929, 614G) displayed enhanced progeny viral production at 33°C compared with 37°C, while SARS-CoV (strain Frankfurt-1) infection was not influenced by temperature (133). The contrasting preferences for pH and temperature exhibited by SARS-CoV and SARS-CoV-2 could be attributed to the stability profiles of their spike proteins under specific environments.

Compared with the nose, the immune responses upon SARS-CoV-2 (strain France/IDF0571/2020, 614D) infection were even more dampened in human primary bronchial epithelial cultures, indicating potential inherent differences in the early immune response to SARS-CoV-2 infection in the human airway (135). Additionally, in primary human tracheobronchial epithelial cells infected with SARS-CoV-2 (München-1.1/2020/929, 614G), a higher IFN-driven innate immune signaling at 37°C than at 33°C was observed. This was accompanied by a higher viral replication at 33°C, raising the question of whether more potent innate immune activation restricted SARS-CoV-2 replication in the human airway at 37°C (133). In the same study, SARS-CoV (strain Frankfurt-1, with ORF8 deletion) infection triggered a weaker type III IFN antiviral and proinflammatory response than did SARS-CoV-2 (133). Nevertheless, in the ex vivo lung tissue, while replicating at a high level, SARS-CoV-2 (HKG/HKU-001a/2020, 614D) showed an impaired induction of interferons and proinflammatory factors compared with SARS-CoV (strain GZ50) (139). These observations indicate that the different replication capability of SARS-CoV and SARS-CoV-2 along the human respiratory tract is not only affected by the variation in their cell entry machinery but also inversely associated with the innate immune response induction during the infection.

4.4.3. Observations in lung models. In postmortem samples of both SARS-CoV infection and SARS-CoV-2 infection, viral antigens were detected in both AT1 and AT2 cells (21–23, 60). In accordance, in human ex vivo tissues, antigens from both viruses were detected in AT1 and AT2 cells, as well as alveolar macrophages (139). Hyperplasia of AT2 cells was reported in the lungs in both SARS-CoV and SARS-CoV-2 fatal infection (21–23, 60).

AT2 cells play a crucial role in lung repair by serving as progenitors for AT1 cells (59). The application of scRNA-seq on COVID-19 patient materials revealed that AT2 cells, as well as AT1 cells, exhibited decreased expression of cell-type identification markers and were apoptotic. These AT2 cells were unable to differentiate into AT1 cells but instead displayed a transient progenitor cell state associated with inflammation. This impaired lung regeneration may contribute to the severity in COVID-19 cases (61, 62). This observation was validated using a 3D AT2 organoid model. In SARS-CoV-2-infected AT2 organoids, expression of AT2-specific surfactant proteins decreased. SARS-CoV-2-positive cells in the organoid culture displayed an elongated

morphology without expressing AT1 markers. The infection with SARS-CoV-2 also resulted in proinflammatory responses and cell death within the AT2 organoids (140, 141).

In SARS-CoV fatal cases, lung cells positive for viruses were identified to belong to a subset with stem/progenitor characteristics, and these cells were missing AT1 and AT2 markers (63). It would be intriguing to investigate whether this particular subset of SARS-CoV-positive lung cells exhibited a similar inflammatory progenitor cell status as observed in COVID-19 patients. While primary AT1 and AT2 cell cultures were established to study SARS-CoV infection (142, 143), the application of novel AT2 organoids as an additional model for SARS-CoV infection is of considerable value.

In both pulmonary cell line Calu-3 cultures and human ex vivo lung tissues, SARS-CoV-2 (strain HKG/HKU-001a/2020, 614D) displayed a higher replication rate and viral production compared with SARS-CoV (strain GZ50), which might be due to the impaired IFNs and proinflammatory responses upon SARS-CoV-2 infection (139, 144). In a multiomics study, SARS-CoV-2 (strain Germany/BavPat1/2020) and SARS-CoV (strain Frankfurt-1) infected lung cell line A549 showed a downregulation of type I IFN and a proinflammatory activation for both virus infections. SARS-CoV infection caused higher activation of the NF-κB pathway, while a specific recruitment of TGFβ factors, which are involved in tissue fibrosis, was observed in SARS-CoV-2 infection. Furthermore, in this study, there was differential regulation of cellular pathways, including ubiquitination and phosphorylation, during SARS-CoV-2 infection compared with SARS-CoV (128). These findings suggest that variations in the cellular machinery employed by SARS-CoV and SARS-CoV-2 may underlie the observed disparities in viral replication kinetics, ultimately impacting the pathogenesis of these two viruses.

Alveolar macrophages and plasmacytoid dendritic cells serve as one of the primary IFN-producing cells during pulmonary infection. Viral antigen–positive macrophages were detected in autopsies in both SARS-CoV and SARS-CoV-2 infections (21, 23). SARS-CoV did not productively infect primary alveolar macrophages, monocyte-derived macrophages, or dendritic cells in vitro. Nevertheless, infection in the lung epithelial cells modulated the intrinsic functions of monocyte-derived macrophages and dendritic cells (142, 145). In the case of SARS-CoV-2, primary alveolar macrophages were not susceptible to productive viral infection and failed in producing IFNs or activating ISGs upon infection (strain 291.3 FR-4286). This finding provided a possible mechanism by which individuals with low-level symptoms may exhibit inactivated immune responses, allowing viral replication in the lungs and eventually contributing to community spreading of SARS-CoV-2 (146).

5. INTEGRATION AND CONCLUSION

The emergence of novel coronaviruses into the human population is almost inevitable, highlighting the importance of understanding the characteristics that contribute to the global pandemic potential of viruses like SARS-CoV-2. The comparative analysis between SARS-CoV and SARS-CoV-2 is therefore crucial for comprehending the pathogenesis of these two highly pathogenic viruses. While studies have contributed to our understanding of disease severity determinants and clinical outcomes, there are limited comparisons of these two viruses under identical experimental conditions.

Animal models have played a crucial role in the broad understanding of the pathological changes upon infections with SARS-CoV and SARS-CoV-2, revealing comparable viral replication kinetics, tissue tropism, shedding, and transmission. However, due to the complex nature of infectious agents like SARS-CoV and SARS-CoV-2, which induce a wide range of clinical manifestations in humans through intricate pathomechanisms, no single animal model can

comprehensively represent all these aspects during infections. Direct comparisons between experimental outcomes in animal models and clinical outcomes in humans are subject to limitations because of variations in the viral entry route and host immune systems, as well as experimental variables. Therefore, animal tissue-derived organoid cultures offer an alternative approach to evaluate the susceptibility of different animal models to SARS-CoV or SARS-CoV-2 infections and the key differences between human and animal hosts, such as the viral receptors and proteases.

Nevertheless, a higher replication of SARS-CoV-2 than SARS-CoV in the nose has been observed in animal models (37), which aligns with clinical observations where viral titers peaked earlier in COVID-19 patients (6, 42, 43). In vitro studies also showed that SARS-CoV-2 replication was favored by pH and temperature conditions resembling those in the human nasal mucosa (125, 133). Impaired intrinsic immune responses in the nasal mucosa may contribute to the increased replication of SARS-CoV-2 (66). Future comparative research is desired to investigate the antiviral immune responses in the nasal mucosa of animals infected with SARS-CoV and SARS-CoV-2. In addition, comparative studies using human nose organoids can provide valuable insights into local immune responses, viral entry mechanisms, and replication fitness of these two viruses in the human nasal mucosa.

The development of ARDS is crucial in determining disease severity and fatality rates. Both SARS-CoV and SARS-CoV-2 have been associated with damages to pulmonary epithelial cells in deceased patients and animal models, which can be a direct cause of ARDS. Single-cell omics have improved the understanding of the disruption in lung repair and regeneration during SARS-CoV-2 infection, revealing an inflammatory state in AT2 cells and their impaired ability to differentiate into AT1 cells. Human AT2 organoids are useful tools for studying this phenomenon. While high-resolution single-cell omics analysis may not be feasible in SARS-CoV clinical autopsies, it can be applied to SARS-CoV-infected AT2 organoids, offering valuable comparative investigations into the lung pathogenesis of SARS-CoV. Furthermore, local inflammatory responses involving immune cells such as macrophages and neutrophils contribute to alveolar damage and immunopathology. Age and male sex are also determinants of the pathogenesis of both SARS-CoV and SARS-CoV-2. Animal models offer valuable opportunities to compare systemic outcomes during infections with these viruses.

The kinetics of viral shedding from the nasal cavity seem to play a crucial role in the pathogenicity of respiratory pathogens. When a novel coronavirus emerges, human nose organoids could facilitate the quick assessment of the potential of the virus to infect and be excreted from the nasal mucosa. Human lung organoids, on the other hand, help to predict the disease impact on the lower respiratory tract, including cellular tropism and innate immune responses. Animal organoid models also aid in determining the susceptibility of experimental animal species to viral infection, guiding the selection of appropriate animal models for studying pathogenesis, disease outcomes, viral shedding, and transmission.

Although adaptive changes were observed in the SARS-CoV viral genome during the outbreak, one common variant predominated during the late phase of the epidemic (147). In contrast, during the SARS-CoV-2 outbreak, several variants of concern of SARS-CoV-2 have been identified, and probably more will be in the near future, with sets of mutations in the spike protein or other sites in the viral genome, which complicate the analysis of their pathogenesis. However, these data will be highly relevant for proper risk assessment not only of these but also of potential new SARS-CoV variants that may emerge in the near future.

DISCLOSURE STATEMENT

The authors are not aware of any affiliations, memberships, funding, or financial holdings that might be perceived as affecting the objectivity of this review.

LITERATURE CITED

1. World Health Organ. 2015. Summary of probable SARS cases with onset of illness from 1 November 2002 to 31 July 2003. World Health Organization. **https://www.who.int/publications/m/item/summary-of-probable-sars-cases-with-onset-of-illness-from-1-november-2002-to-31-july-2003**
2. de Wit E, van Doremalen N, Falzarano D, Munster VJ. 2016. SARS and MERS: recent insights into emerging coronaviruses. *Nat. Rev. Microbiol.* 14:523–34
3. Cui J, Li F, Shi ZL. 2019. Origin and evolution of pathogenic coronaviruses. *Nat. Rev. Microbiol.* 17:181–92
4. Cheng VC, Lau SK, Woo PC, Yuen KY. 2007. Severe acute respiratory syndrome coronavirus as an agent of emerging and reemerging infection. *Clin. Microbiol. Rev.* 20:660–94
5. Zhu N, Zhang D, Wang W, Li X, Yang B, et al. 2020. A novel coronavirus from patients with pneumonia in China, 2019. *N. Engl. J. Med.* 382:727–33
6. Lamers MM, Haagmans BL. 2022. SARS-CoV-2 pathogenesis. *Nat. Rev. Microbiol.* 20:270–84
7. Alwine JC, Casadevall A, Enquist LW, Goodrum FD, Imperiale MJ. 2023. A critical analysis of the evidence for the SARS-CoV-2 origin hypotheses. *mBio* 14:e0058323
8. Pekar JE, Magee A, Parker E, Moshiri N, Izhikevich K, et al. 2022. The molecular epidemiology of multiple zoonotic origins of SARS-CoV-2. *Science* 377:960–66
9. Worobey M, Levy JI, Malpica Serrano L, Crits-Christoph A, Pekar JE, et al. 2022. The Huanan Seafood Wholesale Market in Wuhan was the early epicenter of the COVID-19 pandemic. *Science* 377:951–59
10. Jackson CB, Farzan M, Chen B, Choe H. 2022. Mechanisms of SARS-CoV-2 entry into cells. *Nat. Rev. Mol. Cell Biol.* 23:3–20
11. Du L, He Y, Zhou Y, Liu S, Zheng BJ, Jiang S. 2009. The spike protein of SARS-CoV—a target for vaccine and therapeutic development. *Nat. Rev. Microbiol.* 7:226–36
12. Pinto AL, Rai RK, Brown JC, Griffin P, Edgar JR, et al. 2022. Ultrastructural insight into SARS-CoV-2 entry and budding in human airway epithelium. *Nat. Commun.* 13:1609
13. Wu CT, Lidsky PV, Xiao Y, Cheng R, Lee IT, et al. 2023. SARS-CoV-2 replication in airway epithelia requires motile cilia and microvillar reprogramming. *Cell* 186:112–30.e20
14. Sims AC, Baric RS, Yount B, Burkett SE, Collins PL, Pickles RJ. 2005. Severe acute respiratory syndrome coronavirus infection of human ciliated airway epithelia: role of ciliated cells in viral spread in the conducting airways of the lungs. *J. Virol.* 79:15511–24
15. Sims AC, Burkett SE, Yount B, Pickles RJ. 2008. SARS-CoV replication and pathogenesis in an in vitro model of the human conducting airway epithelium. *Virus Res.* 133:33–44
16. Gu J, Korteweg C. 2007. Pathology and pathogenesis of severe acute respiratory syndrome. *Am. J. Pathol.* 170:1136–47
17. Huang C, Wang Y, Li X, Ren L, Zhao J, et al. 2020. Clinical features of patients infected with 2019 novel coronavirus in Wuhan, China. *Lancet* 395:497–506
18. Rajgor DD, Lee MH, Archuleta S, Bagdasarian N, Quek SC. 2020. The many estimates of the COVID-19 case fatality rate. *Lancet Infect. Dis.* 20:776–77
19. Huang L, Zhang X, Zhang X, Wei Z, Zhang L, et al. 2020. Rapid asymptomatic transmission of COVID-19 during the incubation period demonstrating strong infectivity in a cluster of youngsters aged 16–23 years outside Wuhan and characteristics of young patients with COVID-19: a prospective contact-tracing study. *J. Infect.* 80:e1–13
20. Nicholls JM, Poon LL, Lee KC, Ng WF, Lai ST, et al. 2003. Lung pathology of fatal severe acute respiratory syndrome. *Lancet* 361:1773–78
21. Gu J, Gong E, Zhang B, Zheng J, Gao Z, et al. 2005. Multiple organ infection and the pathogenesis of SARS. *J. Exp. Med.* 202:415–24
22. Bradley BT, Maioli H, Johnston R, Chaudhry I, Fink SL, et al. 2020. Histopathology and ultrastructural findings of fatal COVID-19 infections in Washington State: a case series. *Lancet* 396:320–32
23. Schurink B, Roos E, Radonic T, Barbe E, Bouman CSC, et al. 2020. Viral presence and immunopathology in patients with lethal COVID-19: a prospective autopsy cohort study. *Lancet Microbe* 1:e290–99

24. Roberts A, Vogel L, Guarner J, Hayes N, Murphy B, et al. 2005. Severe acute respiratory syndrome coronavirus infection of golden Syrian hamsters. *J. Virol.* 79:503–11
25. Roberts A, Subbarao K. 2006. Animal models for SARS. *Adv. Exp. Med. Biol.* 581:463–71
26. Roberts A, Lamirande EW, Vogel L, Jackson JP, Paddock CD, et al. 2008. Animal models and vaccines for SARS-CoV infection. *Virus Res.* 133:20–32
27. Chu H, Chan JF, Yuen KY. 2022. Animal models in SARS-CoV-2 research. *Nat. Methods* 19:392–94
28. Rizvi ZA, Dalal R, Sadhu S, Binayke A, Dandotiya J, et al. 2022. Golden Syrian hamster as a model to study cardiovascular complications associated with SARS-CoV-2 infection. *eLife* 11:e73522
29. Muñoz-Fontela C, Dowling WE, Funnell SGP, Gsell PS, Riveros-Balta AX, et al. 2020. Animal models for COVID-19. *Nature* 586:509–15
30. Tiwari S, Goel G, Kumar A. 2022. Natural and genetically-modified animal models to investigate pulmonary and extrapulmonary manifestations of COVID-19. *Int. Rev. Immunol.* **https://doi.org/10.1080/08830185.2022.2089666**
31. Dillard JA, Martinez SA, Dearing JJ, Montgomery SA, Baxter VK. 2023. Animal models for the study of SARS-CoV-2-induced respiratory disease and pathology. *Comp. Med.* 73:72–90
32. Trimpert J, Vladimirova D, Dietert K, Abdelgawad A, Kunec D, et al. 2020. The Roborovski dwarf hamster is a highly susceptible model for a rapid and fatal course of SARS-CoV-2 infection. *Cell Rep.* 33:108488
33. Lawler JV, Endy TP, Hensley LE, Garrison A, Fritz EA, et al. 2006. Cynomolgus macaque as an animal model for severe acute respiratory syndrome. *PLOS Med.* 3:e149
34. Qin C, Wang J, Wei Q, She M, Marasco WA, et al. 2005. An animal model of SARS produced by infection of *Macaca mulatta* with SARS coronavirus. *J. Pathol.* 206:251–59
35. van den Brand JM, Haagmans BL, van Riel D, Osterhaus AD, Kuiken T. 2014. The pathology and pathogenesis of experimental severe acute respiratory syndrome and influenza in animal models. *J. Comp. Pathol.* 151:83–112
36. Blair RV, Vaccari M, Doyle-Meyers LA, Roy CJ, Russell-Lodrigue K, et al. 2021. Acute respiratory distress in aged, SARS-CoV-2-infected African green monkeys but not rhesus macaques. *Am. J. Pathol.* 191:274–82
37. Rockx B, Kuiken T, Herfst S, Bestebroer T, Lamers MM, et al. 2020. Comparative pathogenesis of COVID-19, MERS, and SARS in a nonhuman primate model. *Science* 368:1012–15
38. Martina BE, Haagmans BL, Kuiken T, Fouchier RA, Rimmelzwaan GF, et al. 2003. Virology: SARS virus infection of cats and ferrets. *Nature* 425:915
39. Blanco-Melo D, Nilsson-Payant BE, Liu WC, Uhl S, Hoagland D, et al. 2020. Imbalanced host response to SARS-CoV-2 drives development of COVID-19. *Cell* 181:1036–45.e9
40. Pandey K, Acharya A, Mohan M, Ng CL, Reid SP, Byrareddy SN. 2021. Animal models for SARS-CoV-2 research: a comprehensive literature review. *Transbound. Emerg. Dis.* 68:1868–85
41. Lakdawala SS, Menachery VD. 2020. The search for a COVID-19 animal model. *Science* 368:942–43
42. Peiris JS, Chu CM, Cheng VC, Chan KS, Hung IF, et al. 2003. Clinical progression and viral load in a community outbreak of coronavirus-associated SARS pneumonia: a prospective study. *Lancet* 361:1767–72
43. Cheng PK, Wong DA, Tong LK, Ip SM, Lo AC, et al. 2004. Viral shedding patterns of coronavirus in patients with probable severe acute respiratory syndrome. *Lancet* 363:1699–700
44. Zou L, Ruan F, Huang M, Liang L, Huang H, et al. 2020. SARS-CoV-2 viral load in upper respiratory specimens of infected patients. *N. Engl. J. Med.* 382:1177–79
45. Zhou J, Singanayagam A, Goonawardane N, Moshe M, Sweeney FP, et al. 2023. Viral emissions into the air and environment after SARS-CoV-2 human challenge: a phase 1, open label, first-in-human study. *Lancet Microbe* 4(8):e579–90
46. Khan M, Yoo SJ, Clijsters M, Backaert W, Vanstapel A, et al. 2021. Visualizing in deceased COVID-19 patients how SARS-CoV-2 attacks the respiratory and olfactory mucosae but spares the olfactory bulb. *Cell* 184:5932–49.e15
47. van Doremalen N, Bushmaker T, Morris DH, Holbrook MG, Gamble A, et al. 2020. Aerosol and surface stability of SARS-CoV-2 as compared with SARS-CoV-1. *N. Engl. J. Med.* 382:1564–67

48. Hwang C. 2006. Olfactory neuropathy in severe acute respiratory syndrome: report of a case. *Acta Neurol. Taiwanica* 15:26–28
49. Richard M, Kok A, de Meulder D, Bestebroer TM, Lamers MM, et al. 2020. SARS-CoV-2 is transmitted via contact and via the air between ferrets. *Nat. Commun.* 11:3496
50. Kutter JS, de Meulder D, Bestebroer TM, Lexmond P, Mulders A, et al. 2021. SARS-CoV and SARS-CoV-2 are transmitted through the air between ferrets over more than one meter distance. *Nat. Commun.* 12:1653
51. Kim YI, Yu KM, Koh JY, Kim EH, Kim SM, et al. 2022. Age-dependent pathogenic characteristics of SARS-CoV-2 infection in ferrets. *Nat. Commun.* 13:21
52. Peacock TP, Goldhill DH, Zhou J, Baillon L, Frise R, et al. 2021. The furin cleavage site in the SARS-CoV-2 spike protein is required for transmission in ferrets. *Nat. Microbiol.* 6:899–909
53. Chan JF, Zhang AJ, Yuan S, Poon VK, Chan CC, et al. 2020. Simulation of the clinical and pathological manifestations of coronavirus disease 2019 (COVID-19) in a golden Syrian hamster model: implications for disease pathogenesis and transmissibility. *Clin. Infect. Dis.* 71:2428–46
54. Port JR, Yinda CK, Owusu IO, Holbrook M, Fischer R, et al. 2021. SARS-CoV-2 disease severity and transmission efficiency is increased for airborne compared to fomite exposure in Syrian hamsters. *Nat. Commun.* 12:4985
55. Rockx B, Feldmann F, Brining D, Gardner D, LaCasse R, et al. 2011. Comparative pathogenesis of three human and zoonotic SARS-CoV strains in cynomolgus macaques. *PLOS ONE* 6:e18558
56. Perlman S, Dandekar AA. 2005. Immunopathogenesis of coronavirus infections: implications for SARS. *Nat. Rev. Immunol.* 5:917–27
57. Cameron MJ, Ran L, Xu L, Danesh A, Bermejo-Martin JF, et al. 2007. Interferon-mediated immunopathological events are associated with atypical innate and adaptive immune responses in patients with severe acute respiratory syndrome. *J. Virol.* 81:8692–706
58. Mehta P, McAuley DF, Brown M, Sanchez E, Tattersall RS, Manson JJ. 2020. COVID-19: consider cytokine storm syndromes and immunosuppression. *Lancet* 395:1033–34
59. Planer JD, Morrisey EE. 2023. After the storm: regeneration, repair, and reestablishment of homeostasis between the alveolar epithelium and innate immune system following viral lung injury. *Annu. Rev. Pathol. Mech. Dis.* 18:337–59
60. Nicholls JM, Butany J, Poon LL, Chan KH, Beh SL, et al. 2006. Time course and cellular localization of SARS-CoV nucleoprotein and RNA in lungs from fatal cases of SARS. *PLOS Med.* 3:e27
61. Melms JC, Biermann J, Huang H, Wang Y, Nair A, et al. 2021. A molecular single-cell lung atlas of lethal COVID-19. *Nature* 595:114–19
62. Wang S, Yao X, Ma S, Ping Y, Fan Y, et al. 2021. A single-cell transcriptomic landscape of the lungs of patients with COVID-19. *Nat. Cell Biol.* 23:1314–28
63. Chen Y, Chan VS-F, Zheng B, Chan KY-K, Xu X, et al. 2007. A novel subset of putative stem/progenitor $CD34^{+}Oct\text{-}4^{+}$ cells is the major target for SARS coronavirus in human lung. *J. Exp. Med.* 204:2529–36
64. He L, Ding Y, Zhang Q, Che X, He Y, et al. 2006. Expression of elevated levels of pro-inflammatory cytokines in SARS-CoV-infected $ACE2^{+}$ cells in SARS patients: relation to the acute lung injury and pathogenesis of SARS. *J. Pathol.* 210:288–97
65. Zhang Z, Zheng Y, Niu Z, Zhang B, Wang C, et al. 2021. SARS-CoV-2 spike protein dictates syncytium-mediated lymphocyte elimination. *Cell Death Differ.* 28:2765–77
66. Ziegler CGK, Miao VN, Owings AH, Navia AW, Tang Y, et al. 2021. Impaired local intrinsic immunity to SARS-CoV-2 infection in severe COVID-19. *Cell* 184:4713–33.e22
67. Broggi A, Ghosh S, Sposito B, Spreafico R, Balzarini F, et al. 2020. Type III interferons disrupt the lung epithelial barrier upon viral recognition. *Science* 369:706–12
68. Cameron MJ, Bermejo-Martin JF, Danesh A, Muller MP, Kelvin DJ. 2008. Human immunopathogenesis of severe acute respiratory syndrome (SARS). *Virus Res.* 133:13–19
69. Schaecher SR, Stabenow J, Oberle C, Schriewer J, Buller RM, et al. 2008. An immunosuppressed Syrian golden hamster model for SARS-CoV infection. *Virology* 380:312–21
70. Brocato RL, Principe LM, Kim RK, Zeng X, Williams JA, et al. 2020. Disruption of adaptive immunity enhances disease in SARS-CoV-2-infected Syrian hamsters. *J. Virol.* 94:e01683-20

71. Graham JB, Swarts JL, Leist SR, Schäfer A, Menachery VD, et al. 2021. Baseline T cell immune phenotypes predict virologic and disease control upon SARS-CoV infection in Collaborative Cross mice. *PLOS Pathog.* 17:e1009287
72. Boudewijns R, Thibaut HJ, Kaptein SJF, Li R, Vergote V, et al. 2020. STAT2 signaling restricts viral dissemination but drives severe pneumonia in SARS-CoV-2 infected hamsters. *Nat. Commun.* 11:5838
73. Nouailles G, Wyler E, Pennitz P, Postmus D, Vladimirova D, et al. 2021. Temporal omics analysis in Syrian hamsters unravel cellular effector responses to moderate COVID-19. *Nat. Commun.* 12:4869
74. Sheahan T, Morrison TE, Funkhouser W, Uematsu S, Akira S, et al. 2008. MyD88 is required for protection from lethal infection with a mouse-adapted SARS-CoV. *PLOS Pathog.* 4:e1000240
75. Salvi V, Nguyen HO, Sozio F, Schioppa T, Gaudenzi C, et al. 2021. SARS-CoV-2-associated ssRNAs activate inflammation and immunity via TLR7/8. *JCI Insight* 6:e150542
76. DeDiego ML, Nieto-Torres JL, Regla-Nava JA, Jimenez-Guardeño JM, Fernandez-Delgado R, et al. 2014. Inhibition of NF-κB-mediated inflammation in severe acute respiratory syndrome coronavirus-infected mice increases survival. *J. Virol.* 88:913–24
77. Zheng HY, He XY, Li W, Song TZ, Han JB, et al. 2021. Pro-inflammatory microenvironment and systemic accumulation of $CXCR3^+$ cell exacerbate lung pathology of old rhesus macaques infected with SARS-CoV-2. *Signal. Transduct. Target. Ther.* 6:328
78. Lin X, Fu B, Xiong Y, Xing N, Xue W, et al. 2023. Unconventional secretion of unglycosylated ORF8 is critical for the cytokine storm during SARS-CoV-2 infection. *PLOS Pathog.* 19:e1011128
79. Yu P, Qi F, Xu Y, Li F, Liu P, et al. 2020. Age-related rhesus macaque models of COVID-19. *Anim. Model Exp. Med.* 3:93–97
80. Rosa BA, Ahmed M, Singh DK, Choreño-Parra JA, Cole J, et al. 2021. IFN signaling and neutrophil degranulation transcriptional signatures are induced during SARS-CoV-2 infection. *Commun. Biol.* 4:290
81. Muñoz-Fontela C, Widerspick L, Albrecht RA, Beer M, Carroll MW, et al. 2022. Advances and gaps in SARS-CoV-2 infection models. *PLOS Pathog.* 18:e1010161
82. Wang A, Chiou J, Poirion OB, Buchanan J, Valdez MJ, et al. 2020. Single-cell multiomic profiling of human lungs reveals cell-type-specific and age-dynamic control of SARS-CoV2 host genes. *eLife* 9:e62522
83. Schuler BA, Habermann AC, Plosa EJ, Taylor CJ, Jetter C, et al. 2021. Age-determined expression of priming protease TMPRSS2 and localization of SARS-CoV-2 in lung epithelium. *J. Clin. Investig.* 131:e140766
84. Baas T, Roberts A, Teal TH, Vogel L, Chen J, et al. 2008. Genomic analysis reveals age-dependent innate immune responses to severe acute respiratory syndrome coronavirus. *J. Virol.* 82:9465–76
85. Chen J, Lau YF, Lamirande EW, Paddock CD, Bartlett JH, et al. 2010. Cellular immune responses to severe acute respiratory syndrome coronavirus (SARS-CoV) infection in senescent BALB/c mice: $CD4^+$ T cells are important in control of SARS-CoV infection. *J. Virol.* 84:1289–301
86. Yuan L, Zhu H, Zhou M, Ma J, Chen R, et al. 2021. Gender associates with both susceptibility to infection and pathogenesis of SARS-CoV-2 in Syrian hamster. *Signal. Transduct. Target Ther.* 6:136
87. Dhakal S, Ruiz-Bedoya CA, Zhou R, Creisher PS, Villano JS, et al. 2021. Sex differences in lung imaging and SARS-CoV-2 antibody responses in a COVID-19 golden Syrian hamster model. *mBio* 12:e0097421
88. Francis ME, Richardson B, Goncin U, McNeil M, Rioux M, et al. 2021. Sex and age bias viral burden and interferon responses during SARS-CoV-2 infection in ferrets. *Sci. Rep.* 11:14536
89. Gralinski LE, Bankhead A 3rd, Jeng S, Menachery VD, Proll S, et al. 2013. Mechanisms of severe acute respiratory syndrome coronavirus-induced acute lung injury. *mBio* 4:e00271-13
90. Cross RW, Agans KN, Prasad AN, Borisevich V, Woolsey C, et al. 2020. Intranasal exposure of African green monkeys to SARS-CoV-2 results in acute phase pneumonia with shedding and lung injury still present in the early convalescence phase. *Virol. J.* 17:125
91. Qin Z, Liu F, Blair R, Wang C, Yang H, et al. 2021. Endothelial cell infection and dysfunction, immune activation in severe COVID-19. *Theranostics* 11:8076–91
92. Suresh V, Mohanty V, Avula K, Ghosh A, Singh B, et al. 2021. Quantitative proteomics of hamster lung tissues infected with SARS-CoV-2 reveal host factors having implication in the disease pathogenesis and severity. *FASEB J.* 35:e21713

93. Kuba K, Imai Y, Rao S, Gao H, Guo F, et al. 2005. A crucial role of angiotensin converting enzyme 2 (ACE2) in SARS coronavirus-induced lung injury. *Nat. Med.* 11:875–79
94. Yamaguchi T, Hoshizaki M, Minato T, Nirasawa S, Asaka MN, et al. 2021. ACE2-like carboxypeptidase B38-CAP protects from SARS-CoV-2-induced lung injury. *Nat. Commun.* 12:6791
95. Damas J, Hughes GM, Keough KC, Painter CA, Persky NS, et al. 2020. Broad host range of SARS-CoV-2 predicted by comparative and structural analysis of ACE2 in vertebrates. *PNAS* 117:22311–22
96. Nieto-Torres JL, DeDiego ML, Verdiá-Báguena C, Jimenez-Guardeño JM, Regla-Nava JA, et al. 2014. Severe acute respiratory syndrome coronavirus envelope protein ion channel activity promotes virus fitness and pathogenesis. *PLOS Pathog.* 10:e1004077
97. Jimenez-Guardeño JM, Nieto-Torres JL, DeDiego ML, Regla-Nava JA, Fernandez-Delgado R, et al. 2014. The PDZ-binding motif of severe acute respiratory syndrome coronavirus envelope protein is a determinant of viral pathogenesis. *PLOS Pathog.* 10:e1004320
98. Honrubia JM, Gutierrez-Álvarez J, Sanz-Bravo A, González-Miranda E, Muñoz-Santos D, et al. 2023. SARS-CoV-2-mediated lung edema and replication are diminished by cystic fibrosis transmembrane conductance regulator modulators. *mBio* 14:e0313622
99. Xia B, Shen X, He Y, Pan X, Liu FL, et al. 2021. SARS-CoV-2 envelope protein causes acute respiratory distress syndrome (ARDS)-like pathological damages and constitutes an antiviral target. *Cell Res.* 31:847–60
100. Pfefferle S, Krähling V, Ditt V, Grywna K, Mühlberger E, Drosten C. 2009. Reverse genetic characterization of the natural genomic deletion in SARS-coronavirus strain Frankfurt-1 open reading frame 7b reveals an attenuating function of the 7b protein in-vitro and in-vivo. *Virol. J.* 6:131
101. Silvas JA, Vasquez DM, Park JG, Chiem K, Allué-Guardia A, et al. 2021. Contribution of SARS-CoV-2 accessory proteins to viral pathogenicity in K18 human ACE2 transgenic mice. *J. Virol.* 95:e0040221
102. Li W, Moore MJ, Vasilieva N, Sui J, Wong SK, et al. 2003. Angiotensin-converting enzyme 2 is a functional receptor for the SARS coronavirus. *Nature* 426:450–54
103. Hoffmann M, Kleine-Weber H, Schroeder S, Kruger N, Herrler T, et al. 2020. SARS-CoV-2 cell entry depends on ACE2 and TMPRSS2 and is blocked by a clinically proven protease inhibitor. *Cell* 181:271–80.e8
104. Mykytyn AZ, Breugem TI, Geurts MH, Beumer J, Schipper D, et al. 2023. SARS-CoV-2 Omicron entry is type II transmembrane serine protease-mediated in human airway and intestinal organoid models. *J. Virol.* 97:e0085123
105. Lamers MM, Mykytyn AZ, Breugem TI, Wang Y, Wu DC, et al. 2021. Human airway cells prevent SARS-CoV-2 multibasic cleavage site cell culture adaptation. *eLife* 10:e66815
106. Zhou B, Thao TTN, Hoffmann D, Taddeo A, Ebert N, et al. 2021. SARS-CoV-2 spike D614G change enhances replication and transmission. *Nature* 592:122–27
107. Sungnak W, Huang N, Becavin C, Berg M, Queen R, et al. 2020. SARS-CoV-2 entry factors are highly expressed in nasal epithelial cells together with innate immune genes. *Nat. Med.* 26:681–87
108. Brann DH, Tsukahara T, Weinreb C, Lipovsek M, Van den Berge K, et al. 2020. Non-neuronal expression of SARS-CoV-2 entry genes in the olfactory system suggests mechanisms underlying COVID-19-associated anosmia. *Sci. Adv.* 6:eabc5801
109. Muus C, Luecken MD, Eraslan G, Sikkema L, Waghray A, et al. 2021. Single-cell meta-analysis of SARS-CoV-2 entry genes across tissues and demographics. *Nat. Med.* 27:546–59
110. Zhou L, Niu Z, Jiang X, Zhang Z, Zheng Y, et al. 2020. SARS-CoV-2 targets by the pscRNA profiling of ACE2, TMPRSS2 and furin proteases. *iScience* 23:101744
111. Ahn JH, Kim J, Hong SP, Choi SY, Yang MJ, et al. 2021. Nasal ciliated cells are primary targets for SARS-CoV-2 replication in the early stage of COVID-19. *J. Clin. Investig.* 131:e148517
112. Lan J, Ge J, Yu J, Shan S, Zhou H, et al. 2020. Structure of the SARS-CoV-2 spike receptor-binding domain bound to the ACE2 receptor. *Nature* 581:215–20
113. Shang J, Ye G, Shi K, Wan Y, Luo C, et al. 2020. Structural basis of receptor recognition by SARS-CoV-2. *Nature* 581:221–24
114. Wrapp D, Wang N, Corbett KS, Goldsmith JA, Hsieh CL, et al. 2020. Cryo-EM structure of the 2019-nCoV spike in the prefusion conformation. *Science* 367:1260–63

115. Rawat P, Jemimah S, Ponnuswamy PK, Gromiha MM. 2021. Why are ACE2 binding coronavirus strains SARS-CoV/SARS-CoV-2 wild and NL63 mild? *Proteins* 89:389–98
116. Lima Neto JX, Vieira DS, de Andrade J, Fulco UL. 2022. Exploring the Spike-hACE 2 residue-residue interaction in human coronaviruses SARS-CoV-2, SARS-CoV, and HCoV-NL63. *J. Chem. Inf. Model.* 62:2857–68
117. Li W, Zhang C, Sui J, Kuhn JH, Moore MJ, et al. 2005. Receptor and viral determinants of SARS-coronavirus adaptation to human ACE2. *EMBO J.* 24:1634–43
118. Mykytyn AZ, Breugem TI, Riesebosch S, Schipper D, van den Doel PB, et al. 2021. SARS-CoV-2 entry into human airway organoids is serine protease-mediated and facilitated by the multibasic cleavage site. *eLife* 10:e66815
119. Johnson BA, Xie X, Bailey AL, Kalveram B, Lokugamage KG, et al. 2021. Loss of furin cleavage site attenuates SARS-CoV-2 pathogenesis. *Nature* 591:293–99
120. Reinke LM, Spiegel M, Plegge T, Hartleib A, Nehlmeier I, et al. 2017. Different residues in the SARS-CoV spike protein determine cleavage and activation by the host cell protease TMPRSS2. *PLOS ONE* 12:e0179177
121. Fraser BJ, Beldar S, Seitova A, Hutchinson A, Mannar D, et al. 2022. Structure and activity of human TMPRSS2 protease implicated in SARS-CoV-2 activation. *Nat. Chem. Biol.* 18:963–71
122. Ou T, Mou H, Zhang L, Ojha A, Choe H, Farzan M. 2021. Hydroxychloroquine-mediated inhibition of SARS-CoV-2 entry is attenuated by TMPRSS2. *PLOS Pathog.* 17:e1009212
123. Buchrieser J, Dufloo J, Hubert M, Monel B, Planas D, et al. 2020. Syncytia formation by SARS-CoV-2-infected cells. *EMBO J.* 39:e106267
124. Beucher G, Blondot ML, Celle A, Pied N, Recordon-Pinson P, et al. 2022. Bronchial epithelia from adults and children: SARS-CoV-2 spread via syncytia formation and type III interferon infectivity restriction. *PNAS* 119:e2202370119
125. Laporte M, Raeymaekers V, Van Berwaer R, Vandeput J, Marchand-Casas I, et al. 2021. The SARS-CoV-2 and other human coronavirus spike proteins are fine-tuned towards temperature and proteases of the human airways. *PLOS Pathog.* 17:e1009500
126. Fuentes-Prior P. 2021. Priming of SARS-CoV-2 S protein by several membrane-bound serine proteinases could explain enhanced viral infectivity and systemic COVID-19 infection. *J. Biol. Chem.* 296:100135
127. Gordon DE, Hiatt J, Bouhaddou M, Rezelj VV, Ulferts S, et al. 2020. Comparative host-coronavirus protein interaction networks reveal pan-viral disease mechanisms. *Science* 370(6521):eabe940
128. Stukalov A, Girault V, Grass V, Karayel O, Bergant V, et al. 2021. Multilevel proteomics reveals host perturbations by SARS-CoV-2 and SARS-CoV. *Nature* 594:246–52
129. Huang J, Hume AJ, Abo KM, Werder RB, Villacorta-Martin C, et al. 2020. SARS-CoV-2 infection of pluripotent stem cell-derived human lung alveolar type 2 cells elicits a rapid epithelial-intrinsic inflammatory response. *Cell Stem Cell* 27:962–73.e7
130. Lamers MM, van der Vaart J, Knoops K, Riesebosch S, Breugem TI, et al. 2021. An organoid-derived bronchioalveolar model for SARS-CoV-2 infection of human alveolar type II-like cells. *EMBO J.* 40:e105912
131. Li C, Huang J, Yu Y, Wan Z, Chiu MC, et al. 2023. Human airway and nasal organoids reveal escalating replicative fitness of SARS-CoV-2 emerging variants. *PNAS* 120:e2300376120
132. Muth D, Corman VM, Roth H, Binger T, Dijkman R, et al. 2018. Attenuation of replication by a 29 nucleotide deletion in SARS-coronavirus acquired during the early stages of human-to-human transmission. *Sci. Rep.* 8:15177
133. V'Kovski P, Gultom M, Kelly JN, Steiner S, Russeil J, et al. 2021. Disparate temperature-dependent virus-host dynamics for SARS-CoV-2 and SARS-CoV in the human respiratory epithelium. *PLOS Biol.* 19:e3001158
134. Chua RL, Lukassen S, Trump S, Hennig BP, Wendisch D, et al. 2020. COVID-19 severity correlates with airway epithelium-immune cell interactions identified by single-cell analysis. *Nat. Biotechnol.* 38:970–79
135. Pizzorno A, Padey B, Julien T, Trouillet-Assant S, Traversier A, et al. 2020. Characterization and treatment of SARS-CoV-2 in nasal and bronchial human airway epithelia. *Cell Rep. Med.* 1:100059

136. Hatton CF, Botting RA, Duenas ME, Haq IJ, Verdon B, et al. 2021. Delayed induction of type I and III interferons mediates nasal epithelial cell permissiveness to SARS-CoV-2. *Nat. Commun.* 12:7092
137. Jia HP, Look DC, Shi L, Hickey M, Pewe L, et al. 2005. ACE2 receptor expression and severe acute respiratory syndrome coronavirus infection depend on differentiation of human airway epithelia. *J. Virol.* 79:14614–21
138. Fang Y, Liu H, Huang H, Li H, Saqi A, et al. 2020. Distinct stem/progenitor cells proliferate to regenerate the trachea, intrapulmonary airways and alveoli in COVID-19 patients. *Cell Res.* 30:705–7
139. Chu H, Chan JF, Wang Y, Yuen TT, Chai Y, et al. 2020. Comparative replication and immune activation profiles of SARS-CoV-2 and SARS-CoV in human lungs: an ex vivo study with implications for the pathogenesis of COVID-19. *Clin. Infect. Dis.* 71:1400–9
140. Katsura H, Sontake V, Tata A, Kobayashi Y, Edwards CE, et al. 2020. Human lung stem cell-based alveolospheres provide insights into SARS-CoV-2-mediated interferon responses and pneumocyte dysfunction. *Cell Stem Cell* 27:890–904.e8
141. Mulay A, Konda B, Garcia G Jr., Yao C, Beil S, et al. 2021. SARS-CoV-2 infection of primary human lung epithelium for COVID-19 modeling and drug discovery. *Cell Rep.* 35:109055
142. Mossel EC, Wang J, Jeffers S, Edeen KE, Wang S, et al. 2008. SARS-CoV replicates in primary human alveolar type II cell cultures but not in type I-like cells. *Virology* 372:127–35
143. Qian Z, Travanty EA, Oko L, Edeen K, Berglund A, et al. 2013. Innate immune response of human alveolar type II cells infected with severe acute respiratory syndrome-coronavirus. *Am. J. Respir. Cell Mol. Biol.* 48:742–48
144. Chu H, Chan JF, Yuen TT, Shuai H, Yuan S, et al. 2020. Comparative tropism, replication kinetics, and cell damage profiling of SARS-CoV-2 and SARS-CoV with implications for clinical manifestations, transmissibility, and laboratory studies of COVID-19: an observational study. *Lancet Microbe* 1:e14–23
145. Yoshikawa T, Hill T, Li K, Peters CJ, Tseng CT. 2009. Severe acute respiratory syndrome (SARS) coronavirus-induced lung epithelial cytokines exacerbate SARS pathogenesis by modulating intrinsic functions of monocyte-derived macrophages and dendritic cells. *J. Virol.* 83:3039–48
146. Dalskov L, Mohlenberg M, Thyrsted J, Blay-Cadanet J, Poulsen ET, et al. 2020. SARS-CoV-2 evades immune detection in alveolar macrophages. *EMBO Rep.* 21:e51252
147. Chin. SARS Mol. Epidemiol. Consort. 2004. Molecular evolution of the SARS coronavirus during the course of the SARS epidemic in China. *Science* 303:1666–69
148. Smits SL, de Lang A, van den Brand JMA, Leijten LM, van IJcken WF, et al. 2010. Exacerbated innate host response to SARS-CoV in aged non-human primates. *PLOS Pathog.* 6:e1000756

Annual Review of Pathology: Mechanisms of Disease

Volume 19, 2024

Contents

Errata

An online log of corrections to *Annual Review of Pathology: Mechanisms of Disease* articles may be found at http://www.annualreviews.org/errata/pathmechdis